CHAPTER 10

OPTICAL FIBERS AND FIBER-OPTIC COMMUNICATIONS

Tom G. Brown
The Institute of Optics
University of Rochester
Rochester, New York

10.1 GLOSSARY

A	open loop gain of receiver amplifier
A	pulse amplitude
a	core radius
a_P	effective pump area
A_{eff}	effective (modal) area of fiber
A_i	cross-sectional area of ith layer
B	data rate
B_n	noise bandwidth of amplifier
c	vacuum velocity of light
D	fiber dispersion (total)
E_i	Young's modulus
e_{LO}, e_S	polarization unit vectors for signal and local oscillator fields
F	tensile loading
F_e	excess noise factor (for APD)
g_B	Brillouin gain
g_R	Raman gain
i_d	leakage current (dark)
I_m	current modulation
$I(r)$	power per unit area guided in single mode fiber
k	Boltzmann's constant
J_m	Bessel function of order m
K_m	modified Bessel function of order m
k_0	vacuum wave vector
l	fiber length

l_0	length normalization factor
L_D	dispersion length
m	Weibull exponent
M	modulation depth
N	order of soliton
n	actual number of detected photons
N_{eff}	effective refractive index
N_p	average number of detected photons per pulse
n_0	core index
n_1	cladding index
$n(r)$	radial dependence of the core refractive index for a gradient-index fiber
P	optical power guided by fiber
P_E	error probability
P_f	probability of fiber failure
P_s	received signal power
P_s	signal power
P_R	power in Raman-shifted mode
P_0	peak power
P_0	peak power of soliton
R	detector responsivity (A/W)
RIN	relative intensity noise
R_L	load resistor
$R(r)$	radial dependence of the electric field
S	failure stress
SNR	signal-to-noise ratio measured in a bandwidth B_n
S_0	location parameter
T	temperature (Kelvin)
t	time
T_0	pulse width
U	normalized pulse amplitude
z	longitudinal coordinate
$Z(z)$	longitudinal dependence of the electric field
α	profile exponent
α_f	frequency chirp
α_R	attenuation of Raman-shifted mode
$\tilde{\beta}$	complex propagation constant
β_1	propagation constant
β_2	dispersion (2d order)
Δ	peak index difference between core and cladding
Δf	frequency deviation

ΔL	change in length of fiber under load
$\Delta\phi$	phase difference between signal and local oscillator
$\Delta\nu$	source spectral width
$\Delta\tau$	time delay induced by strain
ε	strain
η_{HET}	heterodyne efficiency
θ_c	critical angle
$\Theta(\theta)$	azimuthal dependence of the electric field
λ	vacuum wavelength
λ_c	cut-off wavelength
ξ	normalized distance
$\Psi(r, \theta, z)$	scalar component of the electric field
Ψ_S, Ψ_{LO}	normalized amplitude distributions for signal and LO
σ_A^2	amplifier noise
$\sigma_d^2 = 2ei_dB_n$	shot noise due to leakage current
$\sigma_J^2 = \dfrac{4kT}{R_L} B_n$	Johnson noise power
$\sigma_R^2 = R^2P_s^2B_n \times 10^{-(\mathrm{RIN}/10)}$	receiver noise due to source RIN
$\sigma_s^2 = 2eRP_sB_nFe$	signal shot noise
τ	time normalized to moving frame
r, θ, z	cylindrical coordinates in the fiber

10.2 INTRODUCTION

Optical fibers were first envisioned as optical elements in the early 1960s. It was perhaps those scientists well-acquainted with the microscopic structure of the insect eye who realized that an appropriate bundle of optical waveguides could be made to transfer an image, and the first application of optical fibers to imaging was conceived. It was Charles Kao[1] who first suggested the possibility that low-loss optical fibers could be competitive with coaxial cable and metal waveguides for telecommunications applications. It was not, however, until 1970 when Corning Glass Works announced an optical fiber loss less than the benchmark level of 10 dB/km[2,3] that commercial applications began to be realized. The revolutionary concept which Corning incorporated and which eventually drove the rapid development of optical fiber communications was primarily a materials one—it was the realization that low doping levels and very small index changes could successfully guide light for tens of kilometers before reaching the detection limit. The ensuing demand for optical fibers in engineering and research applications spurred further applications. Today we see a tremendous variety of commercial and laboratory applications of optical fiber technology. This chapter will discuss important fiber properties, describe fiber fabrication and chemistry, and discuss materials trends and a few commercial applications of optical fiber.

While it is important, for completeness, to include a treatment of optical fibers in any handbook of modern optics, an exhaustive treatment would fill up many volumes all by itself. Indeed, the topics covered in this chapter have been the subject of monographs, reference books, and textbooks; there is hardly a scientific publisher that has not

published several books on fiber optics. The interested reader is referred to the ''Further Reading'' section at the end of this chapter for additional reference material.

Optical fiber science and technology relies heavily on both geometrical and physical optics, materials science, integrated and guided-wave optics, quantum optics and optical physics, communications engineering, and other disciplines. Interested readers are referred to other chapters within this collection for additional information on many of these topics.

The applications which are discussed in detail in this chapter are limited to information technology and telecommunications. Readers should, however, be aware of the tremendous activity and range of applications for optical fibers in metrology and medicine. The latter, which includes surgery, endoscopy, and sensing, is an area of tremendous technological importance and great recent interest. While the fiber design may be quite different when optimized for these applications, the general principles of operation remain much the same. A list of references which are entirely devoted to optical fibers in medicine is listed in ''Further Reading''.

10.3 PRINCIPLES OF OPERATION

The optical fiber falls into a subset (albeit the most commercially significant subset) of structures known as dielectric optical waveguides. The general principles of optical waveguides are discussed elsewhere in Chap. 6 of Vol. II, ''Integrated Optics''; the optical fiber works on principles similar to other waveguides, with the important inclusion of a cylindrical axis of symmetry. For some specific applications, the fiber may deviate slightly from this symmetry; it is nevertheless fundamental to fiber design and fabrication. Figure 1 shows the generic optical fiber design, with a core of high refractive index surrounded by a low-index cladding. This index difference requires that light from inside the fiber which is incident at an angle greater than the critical angle

$$\theta_c = \sin^{-1}\left(\frac{n_1}{n_0}\right) \tag{1}$$

be totally internally reflected at the interface. A simple geometrical picture appears to allow a continuous range of internally reflected rays inside the structure; in fact, the light (being a wave) must satisfy a self-interference condition in order to be trapped in the waveguide. There are only a finite number of paths which satisfy this condition; these are analogous to the propagating electromagnetic modes of the structure. Fibers which support a large number of modes (these are fibers of large core and large numerical aperture) can be adequately analyzed by the tools of geometrical optics; fibers which support a small

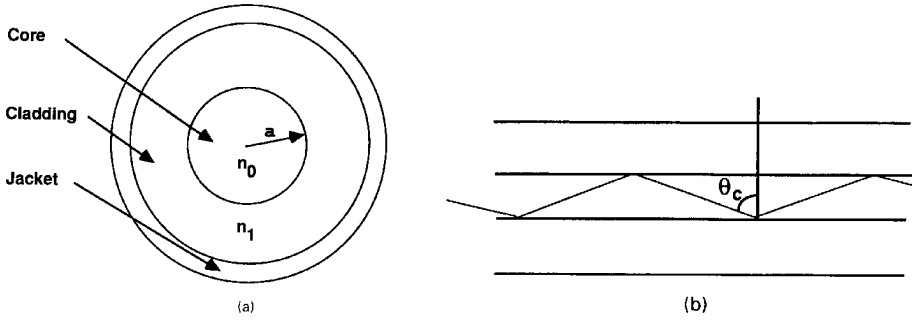

FIGURE 1 (a) Generic optical fiber design, (b) path of a ray propagating at the geometric angle for total internal reflection.

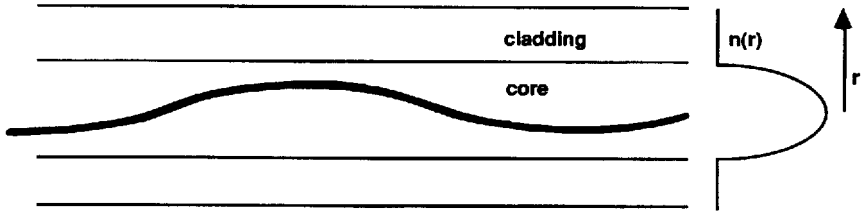

FIGURE 2 Ray path in a gradient-index fiber.

number of modes must be characterized by solving Maxwell's equations with the appropriate boundary conditions for the structure.

Fibers which exhibit a discontinuity in the index of refraction at the boundary between the core and cladding are termed *step-index fibers.* Those designs which incorporate a continuously changing index of refraction from the core to the cladding are termed *gradient-index fibers.* The geometrical ray path in such fibers does not follow a straight line—rather it curves with the index gradient as would a particle in a curved potential (Fig. 2). Such fibers will also exhibit a characteristic angle beyond which light will not internally propagate. A ray at this angle, when traced through the fiber endface, emerges at an angle in air which represents the maximum geometrical acceptance angle for rays *entering* the fiber; this angle is the numerical aperture of the fiber (Fig. 3). Both the core size and numerical aperture are very important when considering problems of fiber-fiber or

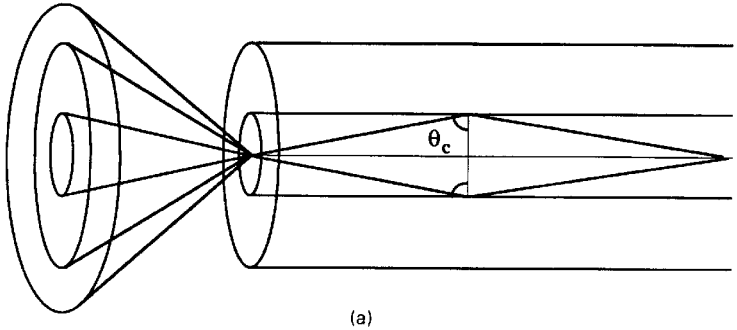

(a)

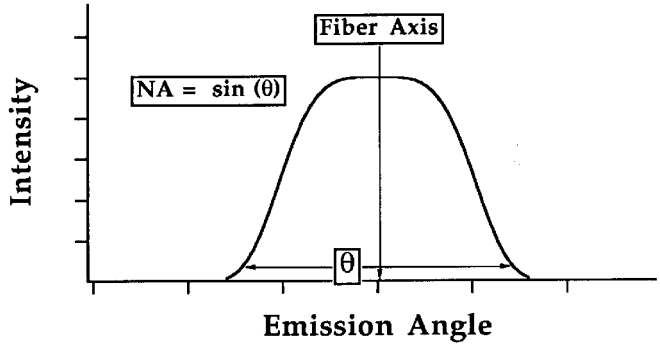

(b)

FIGURE 3 The numerical aperture of the fiber defines the range of external acceptance angles.

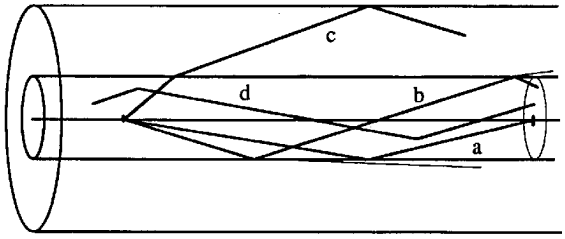

FIGURE 4 Classification of geometrical ray paths in an optical fiber. (*a*) Meridional ray; (*b*) leaky ray; (*c*) ray corresponding to a cladding mode; (*d*) skew ray.

laser-fiber coupling. A larger core and larger numerical aperture will, in general, yield a higher coupling efficiency. Coupling between fibers which are mismatched either in core or numerical aperture is difficult and generally results in excess loss.

The final concept for which a geometrical construction is helpful is ray classification. Those geometrical paths which pass through the axis of symmetry and obey the self-interference condition are known as *meridional rays.* There are classes of rays which are nearly totally internally reflected and may still propagate some distance down the fiber. These are known as *leaky rays* (or modes). Other geometrical paths are not at all confined in the core, but internally reflect off of the cladding-air (or jacket) interface. These are known as *cladding modes.* Finally, there exists a class of geometrical paths which are bound, can be introduced outside of the normal numerical aperture of the fiber, and do not pass through the axis of symmetry. These are often called *skew rays.* Figure 4 illustrates the classification of geometrical paths.

Geometrical optics has a limited function in the description of optical fibers, and the actual propagation characteristics must be understood in the context of guided-wave optics. For waveguides such as optical fibers which exhibit a small change in refractive index at the boundaries, the electric field can be well described by a scalar wave equation,

$$\nabla^2\Psi(r, \theta, z) + k_0^2 r^2(r)\Psi(r, \theta, z) = 0 \tag{2}$$

the solutions of which are the modes of the fiber. $\Psi(r, \theta, z)$ is generally assumed to be separable in the variables of the cylindrical coordinate system of the fiber:

$$\Psi(r, \theta, z) = R(r)\Theta(\theta)Z(z) \tag{3}$$

This separation results in the following eigenvalue equation for the radial part of the scalar field:

$$\frac{d^2R}{dr^2} + \frac{1}{r}\frac{dR}{dr} + \left(k_0^2 n^2(r) - \beta^2 - \frac{m^2}{r^2}\right)R = 0 \tag{4}$$

in which m denotes the azimuthal mode number, and β is the propagation constant. The solutions must obey the necessary continuity conditions at the core-cladding boundary. In addition, guided modes must decay to zero outside the core region. These solutions are readily found for fibers having uniform, cylindrically symmetric regions but require numerical methods for fibers lacking cylindrical symmetry or having an arbitrary index gradient. A common form of the latter is the so-called α-*profile* in which the refractive index exhibits the radial gradient[4]

$$m(r) = \begin{cases} n_1\left[1 - \Delta\left(\dfrac{r}{a}\right)^{\alpha}\right] & r < a \\ n_1[1 - \Delta] = n_2 & r \geq a \end{cases} \tag{5}$$

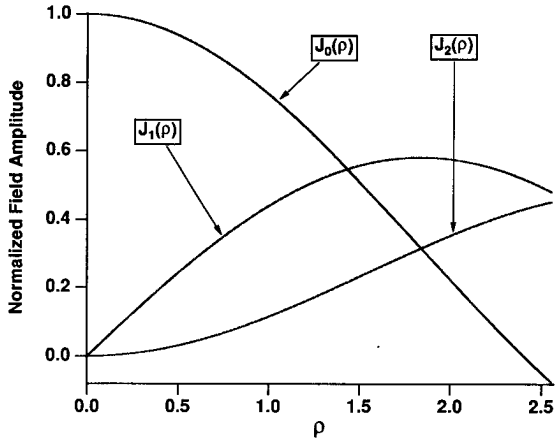

FIGURE 5 Bessel functions $J_m(\rho)$ for $m = 0$, 1, and 2.

The step-index fiber of circular symmetry is a particularly important case, because analytic field solutions are possible and the concept of the "order" of a mode can be illustrated. For this case, the radial dependence of the refractive index is the step function

$$n(r) = \begin{cases} n_1 & r < a \\ n_2 & r \geq a \end{cases} \tag{6}$$

The solutions to this are Bessel functions[5] and are illustrated in Fig. 5. It can be seen that only the lowest-order mode ($m = 0$) has an amplitude maximum at the center. Its solution in the (core) propagating region ($r < a$) is

$$R(r) = \frac{J_0\left((n_1^2 k_0^2 - \beta^2)^{1/2}\left(\frac{r}{a}\right)\right)}{J_0((n_1^2 k_0^2 - \beta^2)^{1/2})} \tag{7}$$

while the solution in the cladding ($r > a$) is the modified Bessel function

$$R(r) = \frac{K_0\left((\beta^2 - n_2^2 k_0^2)^{1/2}\left(\frac{r}{a}\right)\right)}{K_0((\beta^2 - n_2^2 k_0^2)^{1/2})} \tag{8}$$

Higher-order modes will have an increasing number of zero crossings in the cross section of the field distribution.

Fibers which allow more than one bound solution for each polarization are termed *multimode* fibers. Each mode will propagate with its own velocity and have a unique field distribution. Fibers with large cores and high numerical apertures will typically allow many modes to propagate. This often allows a larger amount of light to be transmitted from incoherent sources such as light-emitting diodes (LEDs). It typically results in higher attenuation and dispersion, as discussed in the following section.

By far the most popular fibers for long distance telecommunications applications allow only a single mode of each polarization to propagate. Records for low dispersion and attenuation have been set using single-mode fibers, resulting in length-bandwidth products exceeding 10 Gb-km/s. In order to restrict the guide to single-mode operation, the core diameter must typically be 10 μm or less. This introduces stringent requirements for connectors and splices and increases the peak power density inside the guide. As will be discussed, this property of the single-mode fiber enhances optical nonlinearities which can act to either limit or increase the performance of an optical fiber system.

10.4 FIBER DISPERSION AND ATTENUATION

Attenuation

In most cases, the modes of interest exhibit a complex exponential behavior along the direction of propagation z.

$$Z(z) = \exp(i\tilde{\beta}z) \tag{9}$$

β is generally termed the propagation constant and may be a complex quantity. The real part of β is proportional to the phase velocity of the mode in question, and produces a phase shift on propagation which changes rather rapidly with optical wavelength. It is often expressed as an effective refractive index for the mode by normalizing to the vacuum wave vector:

$$N_{\text{eff}} = \frac{Re\{\tilde{\beta}\}}{k_0} \tag{10}$$

The imaginary part of β represents the loss (or gain) in the fiber and is a weak (but certainly not negligible) function of optical wavelength. Fiber attenuation occurs due to fundamental scattering processes (the most important contribution is Rayleigh scattering), absorption (both the OH-absorption and the long-wavelength vibrational absorption), and scattering due to inhomogeneities arising in the fabrication process. Attenuation limits both the short- and long-wavelength applications of optical fibers. Figure 6 illustrates the attenuation characteristics of a typical fiber.

The variation of the longitudinal propagation velocity with either optical frequency or path length introduces a fundamental limit to fiber communications. Since signaling necessarily requires a nonzero bandwidth, the dispersion in propagation velocity between different frequency components of the signal or between different modes of a multimode fiber produces a signal distortion and intersymbol interference (in digital systems) which is unacceptable. Fiber dispersion is commonly classified as follows.

Intermodal Dispersion

The earliest telecommunications links as well as many modern data communications systems have made use of multimode fiber. These modes (which we have noted have some connection to geometrical ray angles) will typically have a broad range of propagation velocities. An optical pulse which couples to this range of guided modes will tend to broaden by an amount equal to the mean-squared difference in propagation time among

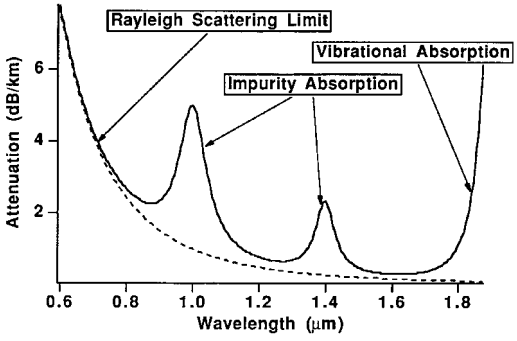

FIGURE 6 Attenuation characteristics of a typical fiber: (*a*) schematic, showing the important mechanisms of fiber attenuation.

the modes. This was the original purpose behind the gradient-index fiber; the geometrical illustrations of Figs 1 and 2 show that, in the case of a step-index fiber, a higher-order mode (one with a steeper geometrical angle or a higher mode index m) will propagate by a longer path than an axial mode. A fiber with a suitable index gradient will support a wide range of modes with nearly the same phase velocity. Vassell was among the first to show this,[6] and demonstrated that a hyperbolic secant profile could very nearly equalize the velocity of all modes. The α-profile description eventually became the most popular due to the analytic expansions it allows (for certain values of α) and the fact that it requires the optimization of only a single parameter.

Multimode fibers are no longer used in long distance (>10 km) telecommunications due to the significant performance advantages offered by single-mode systems. Many short-link applications, for which intermodal dispersion is not a problem, still make use of multimode fibers.

Material Dispersion

The same physical processes which introduce fiber attenuation also produce a refractive index which varies with wavelength. This intrinsic, or material, dispersion is primarily a property of the glass used in the core, although the dispersion of the cladding will influence the fiber in proportion to the fraction of guided energy which actually resides outside the core. Material dispersion is particularly important if sources of broad spectral width are used, but narrow linewidth lasers which are spectrally broadened under modulation also incur penalties from material dispersion. For single-mode fibers, material dispersion must always be considered along with waveguide and profile dispersion.

Waveguide and Profile Dispersion

The energy distribution in a single-mode fiber is a consequence of the boundary conditions at the core-cladding interface, and is therefore a function of optical frequency. A change in frequency will therefore change the propagation constant independent of the dispersion of the core and cladding materials; this results in what is commonly termed *waveguide dispersion.* Since dispersion of the core and cladding materials differs, a change in frequency can result in a small but measurable change in index profile, resulting in *profile dispersion* (this contribution, being small, is often neglected). Material, waveguide, and profile dispersion act together, the waveguide dispersion being of opposite sign to that of the material dispersion. There exists, therefore, a wavelength at which the total dispersion will vanish. Beyond this, the fiber exhibits a region of anomalous dispersion in which the real part of the propagation constant increases with increasing wavelength. Anomalous dispersion has been used in the compression of pulses in optical fibers and to support long distance soliton propagation.

Dispersion, which results in a degradation of the signal with length, combines with attenuation to yield a length limit for a communications link operating at a fixed bandwidth. The bandwidth-length product is often cited as a practical figure of merit which can include the effects of either a dispersion or attenuation limit.

Normalized Variables in Fiber Description

The propagation constant and dispersion of guided modes in optical fibers can be conveniently expressed in the form of normalized variables. Two common engineering problems are the determination of mode content and the computation of total dispersion. For example, commonly available single-mode fibers are designed for a wavelength range

TABLE 1 Normalized Variables in the Mathematical Description of Optical Fibers

Symbol	Description
$k_0 = \dfrac{2\pi}{\lambda}$	Vacuum wave vector
a	Core radius
n_0	Core index
n_1	Cladding index
$\tilde{\beta} = \beta' + i\beta''$	Mode propagation constant
$\alpha = 2\beta''$	Fiber attenuation
$N_{\text{eff}} = \beta'/k_0$	Effective index of mode
$\Delta = \dfrac{n_0^2 - n_1^2}{2n_1^2}$	Normalized core-cladding index differences
$V = \sqrt{2k_0}\, an_1\Delta$	Normalized frequency
$b = \left(\dfrac{N_{\text{eff}}}{n_1} - 1\right)\Big/\Delta$	Normalized effective index
$f(r)$	Gradient-index shape factor
$\Gamma = \dfrac{\int_0^a f(r)\Psi^2(r) r\, dr}{\int_0^a \Psi^2(r) r\, dr}$	Profile parameter ($\Gamma = 1$ for step-index)

of 1.3 to 1.55 μm. Shorter wavelengths will typically support two or more modes, resulting in significant intermodal interference at the output. In order to guarantee single-mode performance, it is important to determine the single-mode cut-off wavelength for a given fiber. Normalized variables allow one to readily determine the cut-off wavelength and dispersion limits of a fiber using universal curves.

The normalized variables are listed in Table 1 along with the usual designations for fiber parameters. The definitions here apply to the limit of the ''weakly guiding'' fiber of Gloge,[7] for which $\Delta \ll 1$. The cutoff for single-mode performance appears at a normalized frequency of $V = 2.405$. For values of V greater than this, the fiber is multimode. The practical range of frequencies for good single-mode fiber operation lie in the range

$$1.8 < V < 2.4 \tag{11}$$

An analytic approximation for the normalized propagation constant b which is valid for this range is given by

$$b(V) \approx \left(1 - 1.1428 - \frac{0.996}{V}\right)^2 \tag{12}$$

Operation close to the cutoff $V = 2.405$ risks introducing higher-order modes if the fiber parameters are not precisely targeted. A useful expression which applies to step-index fibers relates the core diameter and wavelength at the single-mode cutoff[5]:

$$\lambda_{\text{cutoff}} = \left(\frac{\pi}{2.405}\right)(2a)n_0\sqrt{2\Delta} \tag{13}$$

Evaluation of Fiber Dispersion

Evaluation of the fiber dispersion requires:

1. Detailed material dispersion curves such as may be obtained from a Sellmeier formula.[4] The Sellmeier constants for a range of silica-based materials used in fiber fabrication are contained in Chap. 33 of Vol. II, "Crystals and glasses."

2. Complete information about the fiber profile, including compositional as well as refractive index information.

3. Numerical evaluation of the effective indices of the modes in question *and their first and second derivatives.* Several authors have noted the considerable numerical challenge involved in this,[8,9] particularly since measurements of the refractive index/composition possess intrinsic uncertainties.

Figure 7 shows an example of the dispersion exhibited by a step-index single-mode fiber. Different components of the dispersion are shown in order to illustrate the point of zero dispersion near 1.3 μm. The section devoted to fiber properties will describe how profile control can shift the minimum dispersion point to the very low-loss window near 1.55 μm.

10.5 POLARIZATION CHARACTERISTICS OF FIBERS

The cylindrical symmetry of an optical fiber leads to a natural decoupling of the radial and tangential components of the electric field vector. These polarizations are, however, so nearly degenerate that a fiber of circular symmetry is generally described in terms of orthogonal linear polarizations. This near-degeneracy is easily broken by any stresses or imperfections which break the cylindrical symmetry of the fiber. Any such symmetry breaking (which may arise accidentally or be introduced intentionally in the fabrication

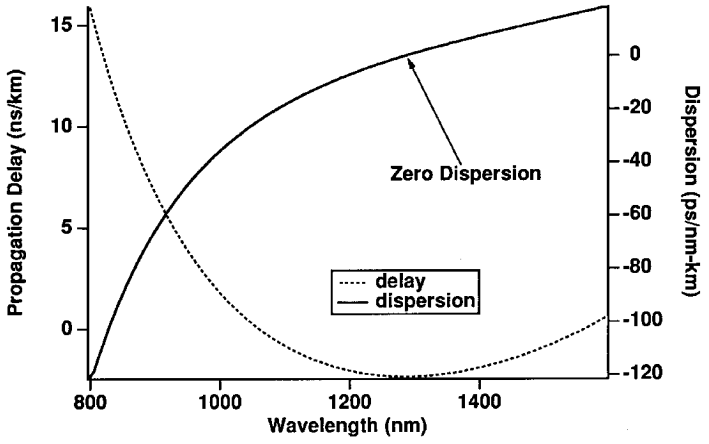

FIGURE 7 Dispersion of a typical single-mode fiber. The opposite contributions of the waveguide and material dispersion cancel near $\lambda = 1.3\ \mu m$. (*Courtesy of Corning, Inc.*)

process) will result in two orthogonally polarized modes with slightly different propagation constants. These two modes need not be linearly polarized; in general, they are two elliptical polarizations. Such polarization splitting is referred to as *birefringence.*

The difference in effective index between the two polarizations results in a state of polarization (SOP) which evolves through various states of ellipticity and orientation. After some propagation distance, the two modes will differ in phase by a multiple of 2π, resulting in a state of polarization identical to that at the input. This characteristic length is called the *beat length* between the two polarizations and is a measure of the intrinsic birefringence in the fiber. The time delay between polarizations is sometimes termed *polarization dispersion,* because it can have an effect on optical communication links which is similar to intermodal dispersion.

If this delay is much less than the coherence time of the source, coherence is maintained and the light in the fiber remains fully polarized. For sources of wide spectral width, however, the delay between the two polarizations may exceed the source coherence time and yield light which emerges from the fiber in a partially polarized or unpolarized state. The orthogonal polarizations then have little or no statistical correlation. The state of polarization of the output can have an important impact on systems with polarizing elements. For links producing an unpolarized output, a 3-dB power loss is experienced when passing through a polarizing element at the output.

The intentional introduction of birefringence can be used to provide polarization stability. An elliptical or double-core geometry will introduce a large birefringence, decoupling a pair of (approximately) linearly polarized modes.[10,11] It also will tend to introduce loss discrimination between modes. This combination of birefringence and loss discrimination is the primary principle behind polarization-maintaining fiber. As will be discussed in the description of optical fiber systems, there is a class of transmission techniques which requires control over the polarization of the transmitted light, and therefore requires polarization-maintaining fiber.

10.6 OPTICAL AND MECHANICAL PROPERTIES OF FIBERS

This section contains brief descriptions of fiber measurement methods and general information on fiber attenuation, dispersion, strength, and reliability. It should be emphasized that nearly all optical and mechanical properties of fibers are functions of chemistry, fabrication process, and transverse structure. Fibers are now well into the commercial arena and specific links between fiber structure, chemistry, and optical and mechanical properties are considered highly proprietary by fiber manufacturers. On the other hand, most fiber measurements now have established standards. We therefore give attention to the generic properties of fibers and the relevant evaluation techniques.

Attenuation Measurement

There are two general methods for the measurement of fiber attenuation. Source-to-fiber coupling must be taken into account in any scheme to measure attenuation, and destructive evaluation accomplishes this rather simply. The *cut-back method*[12,13] for attenuation measurement requires

1. Coupling light into a long length of fiber
2. Measuring the light output into a large area detector (so fiber-detector coupling remains constant)
3. Cutting the fiber back by a known distance and measuring the change in transmitted intensity

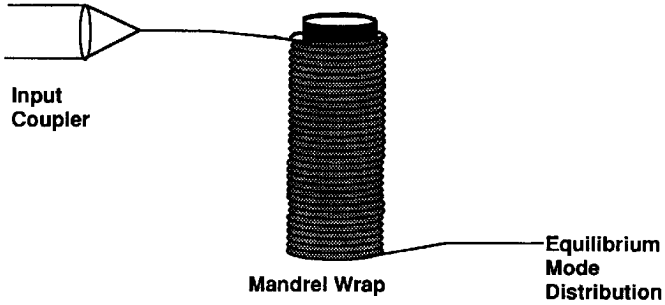

FIGURE 8 Mandrel wrap method of achieving an equilibrium mode distribution.

For single-mode fiber, the fiber can be cut back to a relatively short length provided that the cladding modes are effectively stripped. The concept of ''mode stripping'' is an important one for both attenuation and bandwidth measurements[14] (since modes near or just beyond cutoff can propagate some distance but with very high attenuation). If these modes are included in the measurement, the result yields an anomalously high attenuation. Lossy modes can be effectively stripped by a mandrel wrap or a sufficiently long length of fiber well-matched to the test fiber (see Fig. 8).

For multimode fiber (whether step-index or gradient-index) the excitation conditions are particularly important. This is because the propagating modes of a multimode fiber exhibit widely varying losses. If the laser used for performing the measurement is focused to a tight spot at the center of the core, a group of low-order modes may be initially excited. This group of lower-order modes will have lower loss and the first 10 to 1000 meters will show an anomalously low attenuation. As the propagation distance increases, lower-order modes gradually scatter into higher-order modes and the mode volume ''fills up.'' The high-order modes are substantially lossier, so the actual power flow at equilibrium is that from the lower-order modes to the higher-order and out of the fiber. This process is illustrated in Fig. 9. It is easy to see that if the excitation conditions are set so that all modes guide approximately the same power at the input, the loss in the first hundred meters would be much higher than the equilibrium loss.

With modern single-mode splices, connectors, and couplers, it is sometimes possible to make nondestructive attenuation measurements simply by assuring that the connector loss is much less than the total loss of the fiber length being measured. With this method, care must be taken that the connector design exhibits no interference between fiber endfaces.

Connector loss measurements must have similar control over launch conditions. In addition, it is important to place a sufficiently long length of fiber (or short mandrel wrap) *after* the connector to strip the lossy modes. A slightly misaligned connector will often

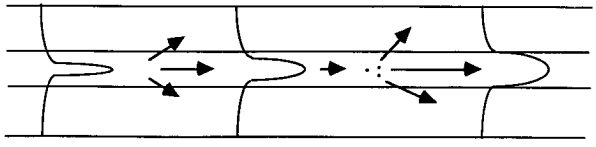

FIGURE 9 In a multimode fiber, low-order modes lose power to the high-order modes, and the high-order modes scatter into cladding and other lossy modes.

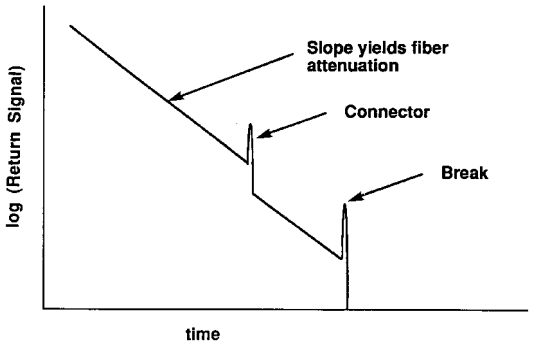

FIGURE 10 Typical OTDR signal. OTDR can be used for attenuation measurement, splice and connector evaluation, and fault location.

exhibit an extremely low loss prior to mode stripping. This is because power is coupled into modes which, while still guided, have high attenuation. It is important, in evaluation of fibers, to properly attribute this loss to the connector and not to the length of fiber which follows.

Another method of nondestructive evaluation of attenuation is optical time domain reflectometry (OTDR). The excitation of a fiber with a narrow laser pulse produces a continuous backscatter signal from the fiber. Assuming a linear and homogeneous scattering process, the reduction in backscattered light with time becomes a map of the round-trip attenuation versus distance. Sudden reductions in intensity typically indicate a splice loss, while a narrow peak will usually indicate a reflection. A typical OTDR signal is shown in Fig. 10. OTDR is extremely sensitive to excitation conditions—a fiber which is not properly excited will often exhibit anomalous behavior. Control of the launch conditions is therefore important for all methods of attenuation measurement.

A major theme of research and development in optical telecommunications has been the elimination of troublesome reflections from optical networks. In particular, high-return loss connectors have been developed which exhibit 30 to 40 dB of reflection suppression.[15–18] OTDR can be used to assess the reflection at network connections as well as perform on-line fault monitoring.

Dispersion and Bandwidth Measurement

The fiber has often been presented as the ''multi-TeraHertz bandwidth transmission channel.'' While it is true that the total attenuation window of the fiber is extremely large by communications standards, the actual information bandwidth at any given wavelength is limited by the various sources of dispersion. The bandwidth of the fiber can be measured either in the time or frequency domain. Both measurements assume the fiber to be linear in its baseband (intensity) transfer characteristics. This assumption breaks down at very high powers and short pulses, but is nevertheless useful in most system applications.

The *time domain measurement*[19] measures the temporal broadening of a narrow input pulse. The ratio of the Fourier transform of the output intensity to that of the input yields a baseband transfer function for the fiber. If the laser and detector are linear, this transfer function relates the drive current of the laser to the photocurrent of the receiver and treats the fiber simply as a linear transmission channel of limited bandwidth. The use of the Fourier transform readily allows the phase to be extracted from the baseband transfer

function. For intermodal pulse broadening in multimode fibers, this phase can be a nonlinear function of frequency, indicating a distortion as well as a broadening of the optical pulse.

Swept-frequency methods[20] have also been used for fiber evaluation. A pure sinusoidal modulation of the input laser is detected and compared in amplitude (and phase, if a network analyzer is available). In principle, this yields a transfer function similar to the pulse method. Both rely on the linearity of the laser for an accurate estimation, but since the swept-frequency method generally uses a single tone, the harmonics produced by laser nonlinearities can be rejected. Agreement between the two methods requires repeatable excitation conditions, a nontrivial requirement for multimode fibers.

The usual bandwidth specification of a multimode fiber is in the form of a 3-dB bandwidth (for a fixed length) or a length-bandwidth product. A single-mode fiber is typically specified simply in terms of the measured total dispersion. This dispersion can be measured either interferometrically, temporally, or using frequency domain techniques.

The *interferometric measurement*[21,22] is appropriate for short fiber lengths, and allows a detailed, direct comparison of the optical phase shifts between a test fiber and a reference arm with a suitable delay. This approach is illustrated in Fig. 11, which makes use of a Mach-Zehnder interferometer. This requires a source which is tunable, and one with sufficient coherence to tolerate small path differences between the two arms. The advantage of the approach is the fact that it allows measurements of extremely small absolute delays (a shift of one optical wavelength represents less than 10 fs time delay). It

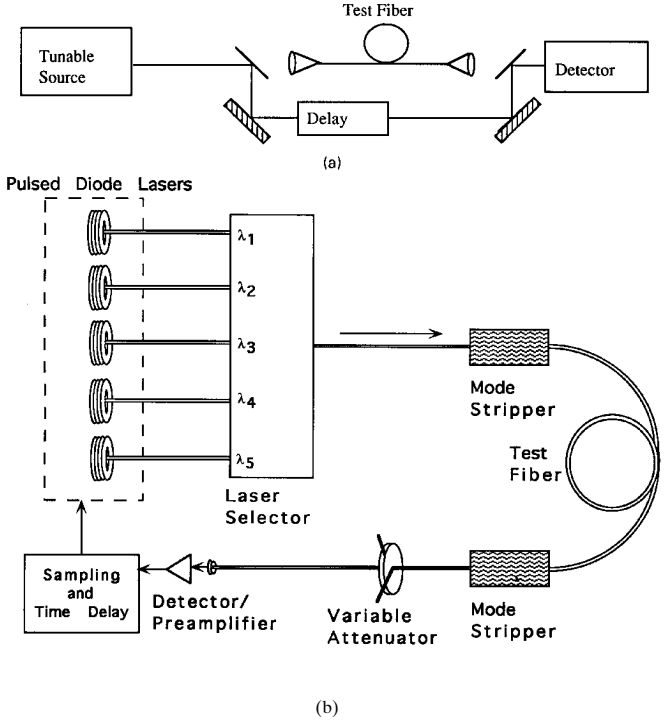

FIGURE 11 (*a*) Interferometric measurement of fiber dispersion; (*b*) time delay measurement of fiber dispersion.

tends to be limited to rather short lengths of fiber; if a fiber is used in the reference arm to balance the interferometer, the properties of that fiber must be known with some accuracy.

Time-domain measurements[23] over a broad spectral range can be made provided a multiwavelength source is available with a sufficiently short optical pulse. One can make use of a series of pulsed diode lasers spaced at different wavelengths, use Raman scattering to generate many wavelengths from a single source, or make use of a tunable, mode-locked solid state laser. The relative delay between neighboring wavelengths yields the dispersion directly. This technique requires fibers long enough to adequately measure the delay, and the optical pulses must be weak enough not to incur additional phase shifts associated with fiber nonlinearities.

Frequency-domain or phase-shift measurements attempt to measure the effects of the dispersion on the baseband signal. A sinusoidally modulated signal will experience a phase shift with propagation delay; that phase shift can be readily measured electronically. This technique uses a filtered broadband source (such as an LED) or a CW, tunable, solid state source to measure the propagation delay as a function of wavelength.

Shifting and Flattening of Fiber Dispersion

A major dilemma facing system designers in the early 1980s was the choice between zero dispersion at 1.3 μm and the loss minimum at 1.55 μm. The loss minimum is an indelible consequence of the chemistry of silica fiber, as is the material dispersion. The waveguide dispersion can, however, be influenced by suitable profile designs.[24] Figure 12 illustrates a generic design which has been successfully used to shift the dispersion minimum to 1.55 μm.

The addition of several core and cladding layers to the fiber design allows for more complicated dispersion compensation to be accomplished. *Dispersion-flattened* fiber is designed for very low dispersion in an entire wavelength range; the spectral region from 1.3 to 1.6 μm is the usual range of interest. This is important for broadband WDM applications, for which the fiber dispersion must be as uniform as possible over a wide spectral region.

Reliability Assessment

The reliability of an optical fiber is of paramount importance in communications applications—long links represent large investments and require high reliability. There will, of course, always be unforeseen reliability problems. Perhaps the most famous such example was the fiber cable design on the first transatlantic link—the designers had not quite appreciated the Atlantic shark's need for a high-fiber diet. The sharks, apparently attracted by the scent of the cable materials, made short work of the initial cable installations. However, most of the stresses which an optical fiber will experience in the field can be replicated in the laboratory. A variety of accelerated aging models (usually relying on temperature as the accelerating factor) can be used to test for active and passive component reliability. In this section, we will review the reliability assessment of the fiber itself, referring interested readers to other sources for information on cable design.

Among the most important mechanical properties of the fiber in a wide range of applications is the tensile strength.[25] The strength is primarily measured destructively, by finding the maximum load just prior to fracture.[26] Full reliability information requires a knowledge of the maximum load, the relation between load and strain, a knowledge of the strain experienced by the fully packaged fiber, and some idea of how the maximum tolerable strain will change over long periods of time. One must finally determine the strain and associated failure probability for fibers with finite bends.

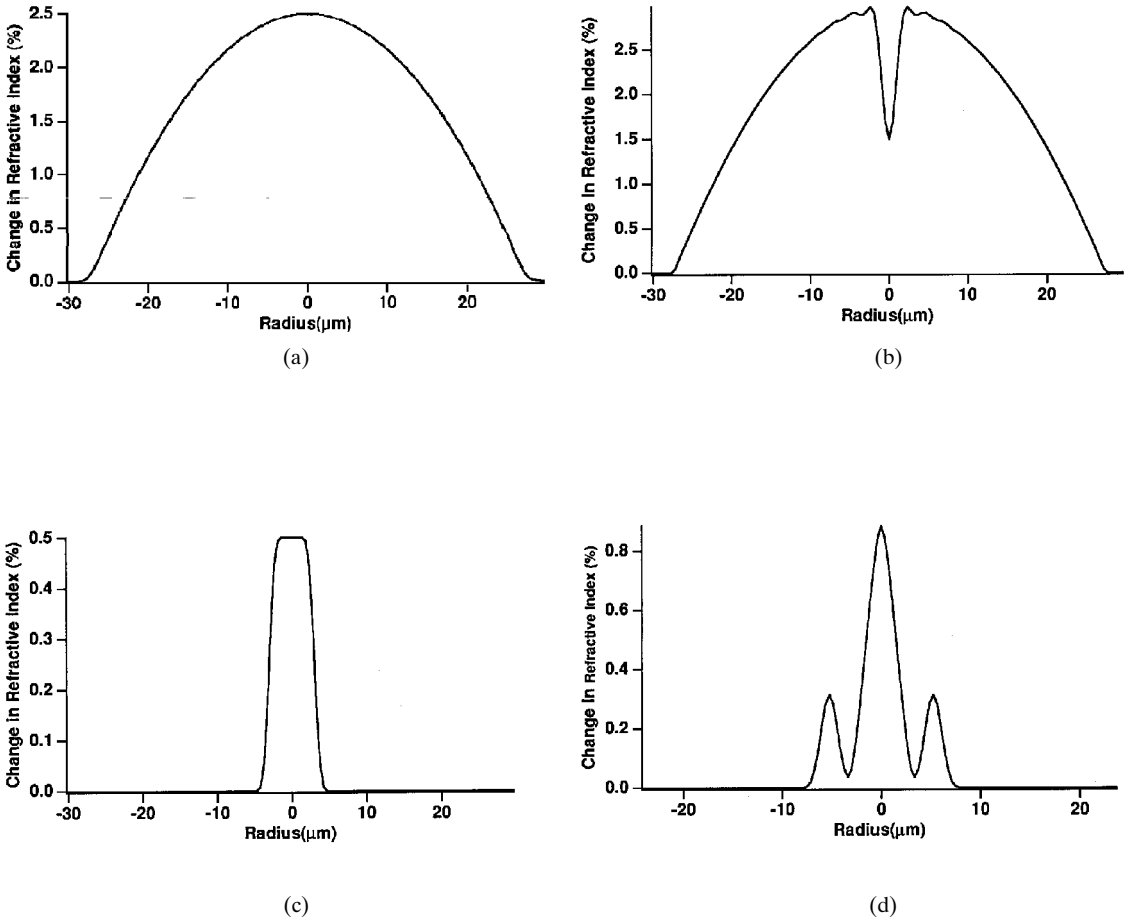

FIGURE 12 Typical index profiles for (*a*), (*b*) gradient-index multimode fiber; (*c*) step-index single-mode fiber; (*d*) dispersion-shifted fiber.

The tensile strength typically decreases slowly over time as the material exhibits fatigue, but in some cases can degrade rather rapidly after a long period of comparative strength. The former behavior is usually linked to fatigue associated with purely mechanical influences, while the latter often indicates chemical damage to the glass matrix. The strain ε and tensile loading F are related through the fiber cross section and Young's modulus:[27]

$$\varepsilon = \frac{F}{\sum_i E_i A_i} \tag{14}$$

E_i and A_i represent the Young's modulus and cross-sectional area of the i_{th} layer of the fiber-jacketing combination. Thus, if the Young's moduli are known, a measurement of the load yields the strain.

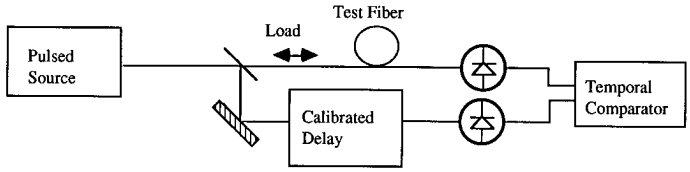

FIGURE 13 Single-pass technique for time-domain measurement of fiber strain.

It is sometimes helpful to measure the fiber strain directly in cases where either the load or Young's moduli are not known. For example, a fiber does not necessarily have a uniform load after jacketing, cabling, and pulling; the load would (in any case) be a difficult quantity to measure. Using the relation between the strain and the optical properties of the fiber it is possible to infer the fiber strain from optical measurements. These techniques have been successful enough to lead to the development of fiber strain gauges for use in mechanical systems.

Optical measurements of strain make use of the transit time of light through a medium of refractive index N_{eff}. (We will, for simplicity, assume single-mode propagation.) A change in length ΔL produced by a strain $\Delta L/L$ will yield a change in transit time

$$\frac{\Delta\tau}{\Delta L} = \frac{N_{\text{eff}}}{c}\left(1 + \frac{L}{N_{\text{eff}}} + \frac{dN_{\text{eff}}}{dL}\right) \tag{15}$$

For most cases of interest, the effective index is simply taken to be the value for that of the core. The ratio $\Delta\tau/\Delta L$ can be calculated (it is about 3.83 ns/m for a germania-silica fiber with $\Delta = 1\%$) or calibrated by using a control fiber and a measured load. It is important to note that this measurement yields only information on the *average* strain of a given fiber length.

There are three categories of optoelectronic techniques for measuring $\Delta\tau$; these are very similar to the approaches for dispersion measurement. A single-pass optical approach generally employs a short-pulse laser source passing through the fiber, with the delay of the transmitted pulse deduced by a comparison with a reference (which presumably is jitter-free). This is shown in Fig. 13. Figure 14*a* shows a multipass optoelectronic scheme, in which an optoelectronic oscillator circuit is set up with the fiber as a delay loop. The Q of the optoelectronic oscillator determines the effective number of passes in this measurement of optical delay. Finally, one can use an all-optical circuit in which the test fiber is placed in a fiber loop with weak optical taps to a laser and detector/signal processor (Fig. 14*b*). This "ring resonator" arrangement can also be set up with a fiber amplifier in the resonator to form the all-optical analog of the multipass optoelectronic scheme of Fig. 14*a*.

If the strain is being used to gain information about fiber reliability, it is necessary to understand how strain, load, and fiber failure are related. Fatigue, the delayed failure of the fiber, appears to be the primary model for fiber failure. One experimental evaluation of this process is to measure the mean time to failure as a function of the load on the fiber with the temperature, the chemical environment, and a host of other factors serving as control parameters.

Since the actual time to failure represents only the average of a performance distribution, the reliability of manufactured fibers is sometimes specified in terms of the two-parameter Weibull distribution[25,27–30]

$$P_f = 1 - \exp\left\{\left(\frac{l}{l_0}\right)\left(\frac{S}{S_0}\right)^m\right\} \tag{16}$$

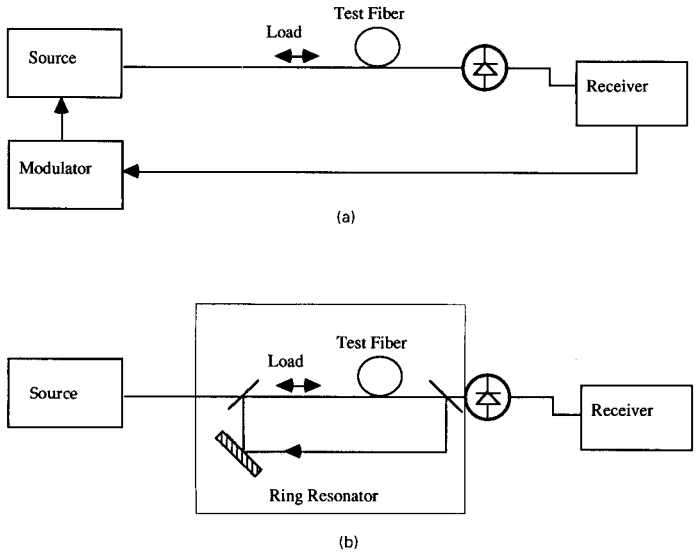

FIGURE 14 Multipass techniques for strain measurement. (*a*) Optoelectronic oscillator; (*b*) optical ring resonator.

where P_f denotes the cumulative failure probability and the parameters are as defined in Table 2. The Weibull exponent m is one of the primary descriptors of long-term fiber reliability. Figure 15 shows a series of Weibull plots associated with both bending and tensile strength measurements for low, intermediate, and high values of m.

One factor which has been shown to have a strong impact on reliability is the absolute humidity of the fiber environment and the ability of the protective coating to isolate the SiO_2 from the effects of H_2O. A recent review by Inniss, Brownlow, and Kurkjian[31] pointed out the correlation between a sudden change in slope, or "knee," in the time-to-failure curve and the H_2O content—a stark difference appeared between liquid and vapor environments. Before this knee, a combination of moisture and stress are required for fiber failure. In the case of fiber environments with a knee, a rather early mean time to failure will exist even for very low fiber stresses, indicating that chemistry rather than mechanical strain is responsible for the failure. The same authors investigated the effects of sodium solutions on the strength and aging of bare silica fibers.

10.7 OPTICAL FIBER COMMUNICATIONS

The optical fiber found its first large-scale application in telecommunications systems. Beginning with the first LED-based systems,[32,34,35] the technology progressed rapidly to longer wavelengths and laser-based systems of repeater lengths over 30 km.[36] The first applications were primarily digital, since source nonlinearities precluded multichannel analog applications. Early links were designed for the 800- to 900-nm window of the optical fiber transmission spectrum, consistent with the emission wavelengths of the GaAs-AlGaAs materials system for semiconductor lasers and LEDs. The development of sources and detectors in the 1.3- to 1.55-μm wavelength range and the further improvement in optical fiber loss over those ranges has directed most applications to either the 1.3-μm window (for low dispersion) or the 1.55-μm window (for minimum loss). The

TABLE 2 Variables Used in the Weibull Distribution

l	Fiber length
l_0	Length normalization factor
S	Failure stress
S_0	Location parameter
m	Weibull exponent

design of dispersion-shifted single-mode fiber along the availability of erbium-doped fiber amplifiers has solidified 1.55 μm as the wavelength of choice for high-speed communications.

The largest currently emerging application for optical fibers is in the local area network (LAN) environment for computer data communications, and the local subscriber loop for telephone, video, and data services for homes and small businesses. Both of these applications place a premium on reliability, connectivity, and economy. While existing systems still use point-to-point optical links as building blocks, there is a considerable range of networking components on the market which allow splitting, tapping, and multiplexing of optical components without the need for optical detection and retransmission.

Point-to-Point Links

The simplest optical communications system is the single-channel (no optical multiplexing) point-to-point digital link. As illustrated in Fig. 16, it consists of a diode laser (with associated driver circuitry and temperature control), optical fiber (with associated splices, connectors, and supporting material), and a detector (with appropriate electronics for signal processing and regeneration). The physics and principles of operation of the laser and detector are covered elsewhere in this collection (see Chap. 11 of Vol. I, ''Lasers'' Chap. 15 of Vol. I, ''Photodetectors''), but the impact of certain device characteristics on the optical fiber communications link is of some importance.

Modulation and Source Characteristics. For information to be accurately transmitted, an appropriate modulation scheme is required. The most common modulation schemes employ direct modulation of the laser drive current, thereby achieving a modulation depth of 80 percent or better. The modulation depth is defined as

$$m = \frac{P_{\max} - P_{\min}}{P_{\max} + P_{\min}} \tag{17}$$

where $P_{\min}$ and $P_{\max}$ are the minimum and maximum laser power, respectively. The modulation depth is limited by the requirement that the laser always remain above threshold, since modulation near the lasing threshold results in a longer turn-on time, a broader spectrum, and higher source noise.

The transmitting laser contributes noise to the system in a fashion that is, generally speaking, proportional to the peak transmitted laser power. This noise is always evaluated as a fraction of the laser power and is therefore termed *relative intensity noise* (RIN). The RIN contribution from a laser is specified in dB/Hz, to reflect a spectral density which is

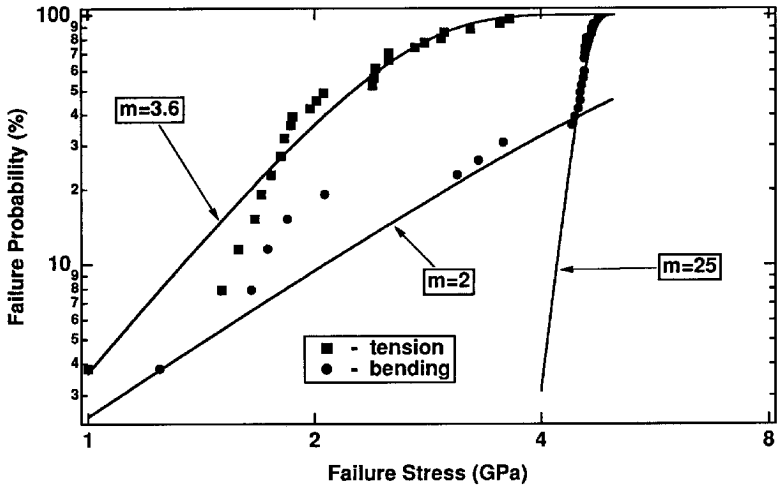

(a)

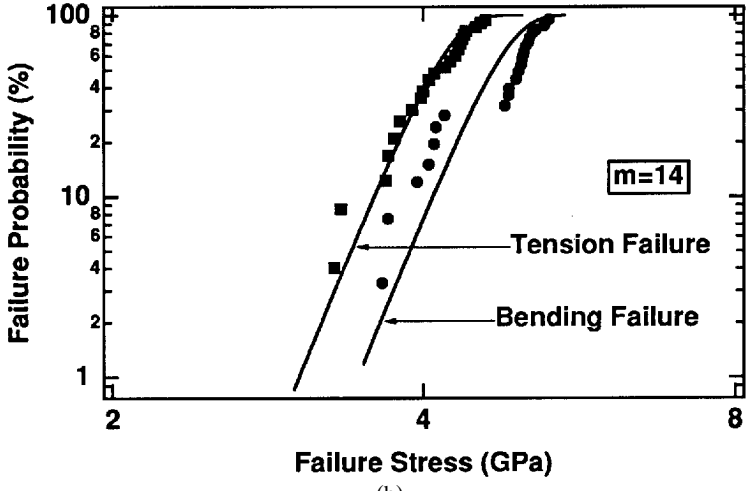

(b)

FIGURE 15 A series of Weibull plots comparing bending and tensile strength for (*a*) low, (*b*) intermediate, and (*c*) high values of the Weibull exponent *m*; (*d*) shows a typical mean time to failure plot. Actual fibers will often exhibit slope discontinuities, indicating a change in the dominant failure mechanism. (Data Courtesy of Corning, Inc.)

approximately flat and at a fixed ratio (expressed in dB) to the laser power. Figure 17 shows a typical plot of the relative intensity noise of a source. The specification of RIN as a flat noise source is valid only at frequencies much less than the relaxation oscillation frequency and in situations where reflections are small.

The relative intensity noise is affected rather dramatically by the environment of the

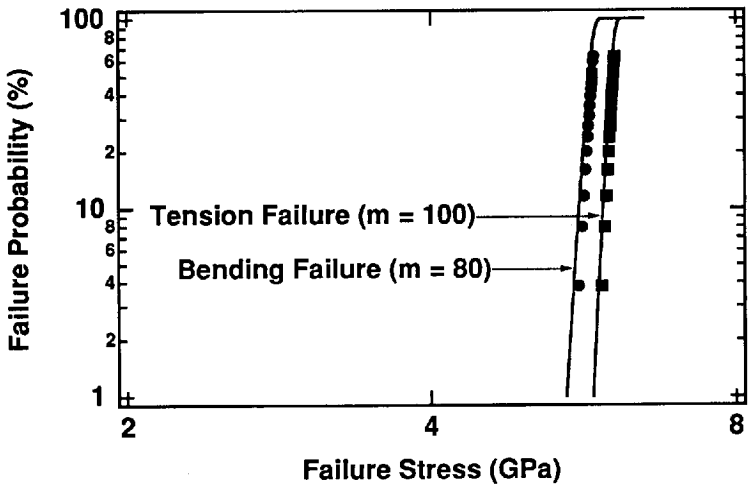

(c)

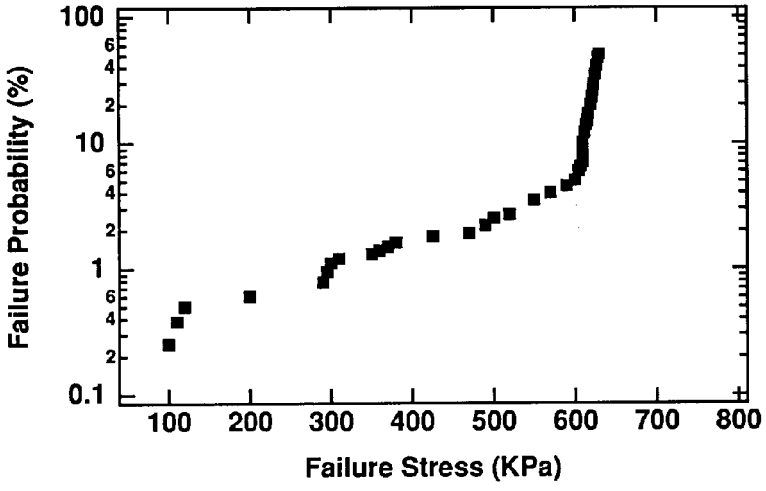

(d)

FIGURE 15 (*Continued*)

diode laser. A rather weak reflection back into the laser will both increase the magnitude of the relative intensity noise and modify its spectrum. As the reflection increases, it can produce self-pulsations and chaos in the output of the laser, rendering it useless for communications applications.[37] Thus, the laser cannot be thought of as an isolated component in the communications system. Just as RF and microwave systems require impedance matching for good performance, an optical communications system must minimize reflections. This is relatively easily accomplished for a long distance telecommunications link which makes use of low-reflection fusion splices. However, in a short

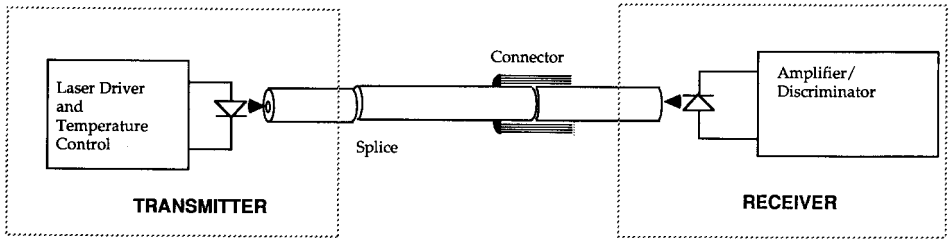

FIGURE 16 Typical point-to-point optical fiber communications link.

link-network environment which must be modular, a small number of connectors can cause severe problems unless those connectors are designed to minimize reflections. It is now widely accepted that optical fiber connectors must be specified both in terms of insertion loss and reflection. A 1 percent reflection from a fiber connector can have far more serious implications for an optical fiber link than a 1 percent loss which is not reflected back to the laser. Optical isolators are available but only at considerable expense and are not generally considered economically realistic for network environments.

Impact of Fiber Properties on a Communications Link. For moderate power levels, the fiber is a passive, dispersive transmission channel. Dispersion can limit system performance in two ways. It results in a spreading of data pulses by an amount proportional to the spectral width of the source. This pulse spreading produces what is commonly termed "intersymbol interference." This should not be confused with an optical interference effect, but is simply the blurring of pulse energy into the neighboring time slot. In simple terms, it can be thought of as a reduction in the modulation depth of the signal as a function of link length. The effects of dispersion are often quantified in the form of a power penalty. This is simply a measure of the additional power required to overcome the effects of the dispersion, or bring the modulated power to what it would be in an identical link without dispersion. It is commonly expressed as a decibel ratio of the power required at the receiver compared to that of the ideal link.

Modulation-induced frequency chirp of the laser source will also result in pulse

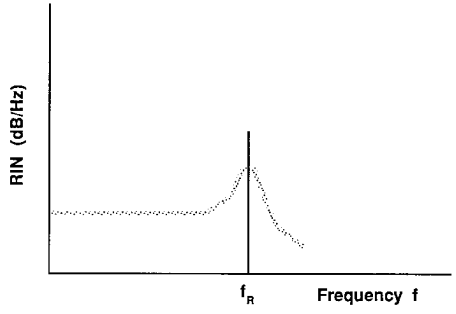

FIGURE 17 Typical RIN spectrum for a diode laser. The peak corresponds to the relaxation resonance frequency, f_R, of the laser.

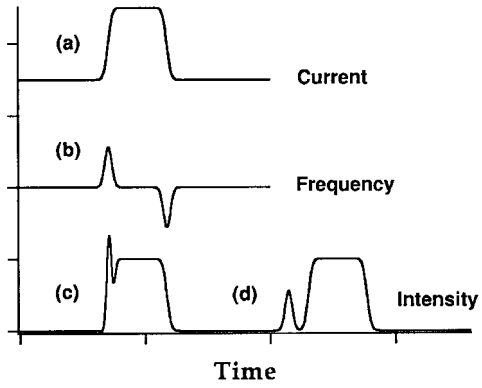

FIGURE 18 Modulation of the drive current in a semiconductor laser (*a*) results in both an intensity (*b*) and a frequency modulation (*c*). The pulse is distorted after transmission through the fiber (*d*).

distortion. This is illustrated in Fig. 18, in which the drive current of the laser is modulated. The accompanying population relaxation produces a frequency modulation of the pulse. Upon transmission through a dispersive link, these portions of the pulse which are "chirped" will be advanced or retarded, resulting in both pulse distortion and intersymbol interference.

System Design. The optical receiver must, within the signal bandwidth, establish an adequate signal-to-noise ratio (SNR) for accurate regeneration/retransmission of the signal. It must accomplish this within the constraints of the fiber dispersion and attenuation, the required system bandwidth, and the available source power. First-order system design normally requires the following steps:

1. Determine the maximum system bandwidth (or data rate for digital systems) and the appropriate transmission wavelength required for the system.

2. Find the maximum source RIN allowable for the system. For analog systems, in which a signal-to-noise ratio (SNR) must be specified in a bandwidth B_n, the RIN (which is usually specified in dB/Hz, indicating a measurement in a 1-Hz bandwidth) must obey the following inequality:

$$|\text{RIN(dB/Hz)}| \ll 10 \log (\text{SNR} \cdot B_n) \tag{18}$$

The SNR is specified here as an absolute ratio of carrier power to noise power. For an SNR specified as a decibel ratio,

$$|\text{RIN(dB/Hz)}| \ll \text{SNR(dB)} + 10 \log (B_n) \tag{19}$$

For digital systems, a Gaussian assumption allows a simple relationship between error probability (also termed bit error rate) and the signal-to-noise ratio:

$$P_E = 0.5 erfc[0.5(0.5\text{SNR})^{1/2}] \tag{20}$$

Where *erfc* denotes the complementary error function and the decision threshold is assumed to be midway between the on and off states. The maximum error probability due to source noise should be considerably less than the eventual target error probability. For

system targets of 10^{-9} to 10^{-12}, the error probability due to source RIN should be considerably less than 10^{-20}. This will allow at least a 3-dB margin to allow for increases in RIN due to device aging.

3. Establish a length limit associated with the source frequency chirp and spectral width. The frequency chirp α_f is specified in GHz per milliampere change in the drive current of the laser. A total current modulation I_m therefore yields a frequency deviation Δf of

$$\Delta f = I_m \alpha_f \tag{21}$$

This frequency deviation translates into a propagation delay via the fiber intramodal dispersion D. This delay must be kept less than the minimum pulse width (data rate). With D specified in ps/nm-km, the length in kilometers must obey the following inequality to avoid penalties due to frequency chirp:

$$L \ll \frac{c}{B\Delta f D\lambda_0^2} = \frac{c}{\alpha_f I_m B D \lambda_0^2} \tag{22}$$

where B denotes the data rate and is the reciprocal of the pulse width for data pulses that fill up an entire time slot. (These signals are designated non-return-to-zero, or NRZ.)

The length limit due to source spectral width $\Delta\nu$ obeys a similar inequality—in this case, the delay associated with the spectral spread of the source must remain much less than one pulse width:

$$L \ll \frac{c}{\Delta\nu B D \lambda_0^2} \tag{23}$$

If the chirp is low and the unmodulated source bandwidth is less than the system bandwidth being considered, one must require that the delay distortion of the signal spectrum itself be small compared to a pulse width, requiring

$$L \ll \frac{c}{B^2 D \lambda_0^2} \tag{24}$$

For multimode fiber systems, the limiting length will generally be associated with the intermodal dispersion rather than the material and waveguide dispersion. A length-bandwidth product is generally quoted for such fibers. With the length and bandwidth limits established, it is now possible to design, within those limits, a receiver which meets the necessary specifications.

4. Determine the minimum power required at the receiver to achieve the target SNR or error probability. This minimum acceptable power (MAP) is first computed assuming an ideal source (no RIN contribution). A correction for the RIN can be carried out later. A computation of the MAP requires a knowledge of the noise sources and detector bandwidth. It is conventional to express the noise sources in terms of equivalent input noise current sources. The noise sources of importance for such systems are: the shot noise of the photocurrent, dark current, and drain current (in the case of a field effect transistor (FET) preamplifier); the Johnson noise associated with the load resistor or equivalent amplifier input impedance; 1/f noise from certain classes of FETs. The noise contributions from amplifiers other than the first stage are generally second-order corrections. Figure 19 shows a schematic of the receiver and relevant noise sources. Table 3 gives expressions for, and definitions of the important physical quantities which determine the receiver sensitivity.

Figure 20 illustrates two possible configurations for the detector/amplifier combination.

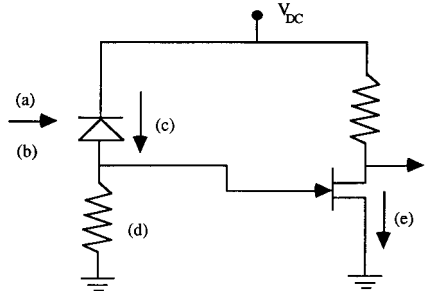

FIGURE 19 Schematic of the receiver, showing the introduction of noise into the system. Noise sources which may be relevant include (*a*) signal shot noise; (*b*) background noise (due to thermal background or channel crosstalk); (*c*) shot noise from the leakage current; (*d*) Johnson noise in the load resistor; (*e*) shot noise and 1/f noise in the drain current of the field effect transistor.

Of these, the integrating front end is the simplest (particularly for high-frequency operation) but tends to be slower than a transimpedance amplifier with an equivalent load resistance. This is because the transimpedance amplifier reduces the effective input impedance of the circuit by $(A + 1)$, where A denotes the open loop gain of the amplifier.

For equivalent bandwidth, the transimpedance amplifier exhibits a lower Johnson noise contribution since a higher feedback resistance is possible. It is worth mentioning that the transimpedance design tends to be much more sensitive to the parasitic capacitance which appears across the feedback resistor—small parasitics across the load resistor tend to be less important for the integrating front end.

The excess noise factor F_e is determined by the choice of detector. There are several choices over the wavelength range generally of interest for optical fiber transmission. (A detailed discussion of the principles of operation can be found in Chaps. 15–17 of Vol. I.)

TABLE 3 Symbols and Expressions for Receiver Noise

Symbol	Description
R_L	Load resistor
k	Boltzmann's constant
T	Temperature (Kelvin)
$\sigma_J^2 = \dfrac{4kT}{R_L} B_n$	Johnson noise power
R	Detector responsivity (A/W)
$P_g P$	Signal power
B_n	Noise bandwidth of amplifier
$\sigma_s^2 = 2eRP_sB_nFe$	Signal shot noise
i_d	Leakage current (dark)
$\sigma_d^2 = 2ei_dB_n$	Shot noise due to leakage current
$\sigma_R^2 = R^2P_s^2B_n \times 10^{-(\mathrm{RIN}/10)}$	Receiver noise due to source RIN
F_e	Excess noise factor (for APD)
σ_λ^2	Amplifier noise

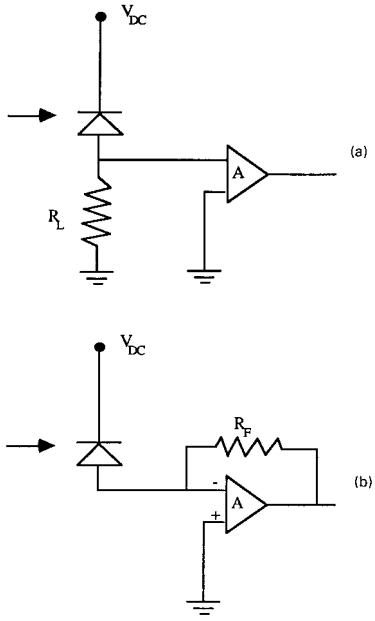

FIGURE 20 Two possible configurations for the detector/amplifier: (*a*) the integrating front end yields the simplest design for high speed operation; (*b*) the transimpedance amplifier provides an expansion of the receiver bandwidth by a factor of $A + 1$, where A is the open loop gain of the amplifier.

1. The p-i-n photodiode is described in some detail in Chap. 15 of Vol. I (''Photodetectors''). It can provide high quantum efficiencies and speeds in excess of 1 GHz. Dark currents range from less than 1 nA for silicon devices to 1 μA or more for Ge diodes. The dark current increases and the device slows down as the active area is increased.

2. The avalanche photodiode is a solid state device which exhibits internal multiplication of the photocurrent in a fashion that is sometimes compared with the gain in photomultiplier tubes. The multiplication does not come without a penalty, however, and that penalty is typically quantified in the form of an excess noise factor which multiplies the shot noise. The excess noise factor is a function both of the gain and the ratio of impact ionization rates between electrons and holes.

Figure 21 shows the excess noise factor for values of k ranging from 50 (large hole multiplication) to 0.03 (large electron multiplication). The former is claimed to be typical of certain III–V compounds while the latter is typical of silicon devices. Germanium, which would otherwise be the clear detector of choice for long wavelengths, has the unfortunate property of having k near unity. This results in maximum excess noise, and Ge avalanche photodiodes must typically be operated at low voltages and relatively small gains. The choice of a p-i-n detector, which exhibits no internal gain, yields $F_e = 1$.

3. The need for very high speed detectors combined with the fabrication challenges present in III-V detector technology has led to a renewed interest in Schottky barrier detectors for optical communications. A detector of considerable importance today is the metal-semiconductor-metal detector, which can operate at extremely high speed in an

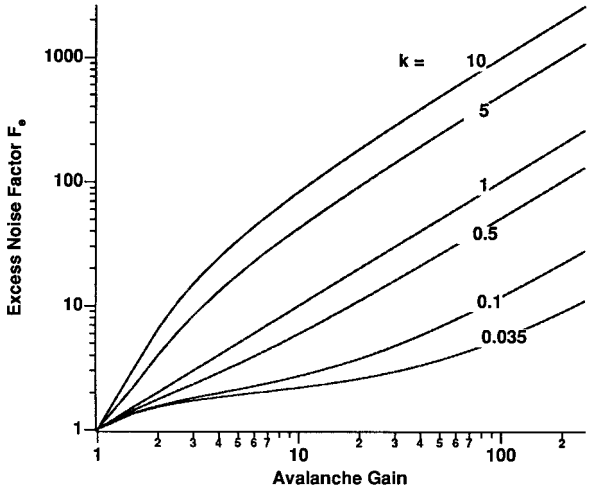

FIGURE 21 Excess noise factor for an avalanche photodiode with the electron/hole multiplication ratio k as a parameter. Small values of k indicate purely electron multiplication while large values of k indicate purely hole multiplication.

interdigitated electrode geometry. Chapter 17 of Vol. I provides further discussion of MSM detectors.

With all noise sources taken into account (see Table 3 for the relevant expressions), the signal-to-noise ratio of an optical receiver can be expressed as follows:

$$\mathrm{SNR} = \frac{R^2 P_S^2}{\sigma_S^2 + \sigma_T^2} \tag{25}$$

where σ_T^2 denotes the total signal-independent receiver noise:

$$\sigma_T^2 = \sigma_D^2 + \sigma_J^2 + \sigma_A^2 \tag{26}$$

and σ_S^2 is the signal shot noise as in Table 3. If the effects of RIN are to be included, the following correction to the SNR may be made:

$$\mathrm{SNR}^{-1} = \mathrm{SNR}^{-1} + \sigma_R^2 \tag{27}$$

With the signal-to-noise ratio determined, the error probability may be expressed in terms of the signal-to-noise ratio

$$P_E = 0.5 erfc[0.5(0.5 \times \mathrm{SNR})^{1/2}] \tag{28}$$

The above expressions assume Gaussian distributed noise sources. This is a good assumption for nearly all cases of interest. The one situation in which the Gaussian assumption underestimates the effects of noise is for avalanche photodiodes with large excess noise. It was shown by McIntyre[38,39] and Personick[40] that the avalanche multiplication statistics are skewed and that the Gaussian assumption yields overly optimistic results.

5. Given the MAP of the receiver, the fiber attenuation and splice loss budget, and the available pigtailed laser power (the maximum power coupled into the first length of fiber by the laser), it is possible to calculate a link loss budget. The budget must include a substantial power margin to allow for device aging, imperfect splices, and a small measure of stupidity. The result will be a link length which, if shorter than the dispersion limit, will provide an adequate signal-to-noise ratio.

For further link modeling, a variety of approaches can be used to numerically simulate the link performance and fully include the effects of fiber dispersion, a realistic detector-preamplifier combination, and a variety of other factors which the first-order design does not include. Nevertheless, a first-order design is necessary to reduce the range of free parameters used in the simulation.

The ultimate goal of the point-to-point link is to transparently transmit the data (or the analog signal) in such a way that standard communications techniques may be used in the optical link. Examples include the use of block or error-correcting codes in digital systems, standard protocols for point-to-point links between nodes of a network, or frequency allocation in the case of a multichannel analog link.

Advanced Transmission Techniques

The optical bandwidth available in either of the low-loss transmission windows of the fiber exceeds 10^{13} Hz. Two ways of taking full advantage of this bandwidth are through the use of ultrashort pulse transmission combined with time-division multiplexing or the use of wavelength/frequency-division multiplexing. Either technique can overcome the limits imposed by the channel dispersion, but both techniques have their limitations. The first technique seeks to turn fiber dispersion to advantage; the second attempts to simply reduce the negative effects of dispersion on a broadband optical signal.

Ultrashort Pulse Transmission. The most common form of multiplexing in digital communication systems is the combination of a number of low data rate signals into a single, high data rate signal by the use of time-division multiplexing. This requires much shorter optical pulses than are used in conventional transmission. As mentioned earlier, the normal (linear) limitation to the data rate is imposed by the fiber attenuation and dispersion. Both of these limits can be exceeded by the use of soliton transmission and optical amplification.

The physics of soliton formation[41–45] is discussed in ''Nonlinear Optical Properties of Fibers,'' later in this chapter. Solitons, in conjunction with fiber amplifiers, have been shown to promise ultralong distance transmission without the need for optoelectronic repeaters/regenerators. Time-division multiplexing of optical solitons offers the possibility of extremely long distance repeaterless communications.

No communication technique is noise-free, and even solitons amplified by ideal amplifiers will exhibit phase fluctuations which broaden the spectrum and eventually cause the soliton to break up. This spontaneous-emission noise limit is known as the Gordon-Haus limit,[46] and had been thought to place a rather severe upper limit on the bit rate distance product for optical fiber systems. It has recently been noted,[47] that a unique series of linear filters can prevent the buildup of unwanted phase fluctuations in the soliton, thereby justifying amplified soliton transmission as a viable technology for undersea communications.

Such a communications system puts great demands on the signal processing both at the input and the output. For very high bit rates, one needs either all-optical demultiplexing or extremely fast electronic logic. Current limits on silicon logic are in the range of several

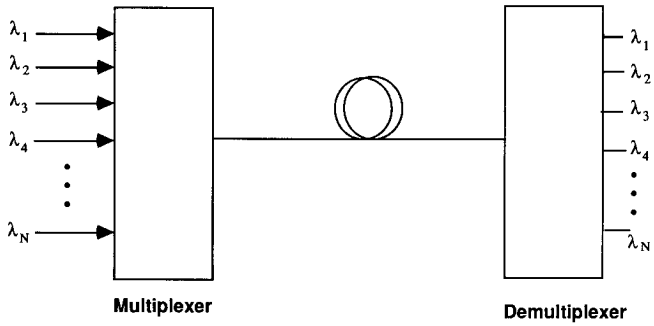

FIGURE 22 Schematic of a WDM transmission system. The main figures of merit are insertion loss (for both the multiplexer and demultiplexer) and channel crosstalk (for the demultiplexer).

Gb/s, which may be adequate for the first implementations of soliton transmission. It is anticipated that all-optical multiplexing and demultiplexing will be required in order to fully exploit the optical fiber bandwidth.

Solitons supported by an optical fiber bear a very specific relationship between pulse width T_0, peak power P_0, fiber dispersion D, effective area A_{eff}, and the intensity-dependent refractive index n_2. For a lowest-order ($N = 1$) soliton,

$$T_0^2 = \frac{\lambda^3 D}{(2\pi)^2 n_2 (P_0/A_{\text{eff}})} \tag{29}$$

Under normal operation, a fiber will propagate lowest-order solitons of about 10 ps in duration. Even for a pulse train of comparatively high duty cycle, this represents less than 100 GHz of a much larger fiber bandwidth. To fully span the bandwidth requires wavelength-division multiplexing.

Wavelength-division Multiplexing (WDM). The troublesome delay between frequencies which is introduced by the fiber dispersion can also be overcome by division of the fiber transmission region into mutually incoherent (uncorrelated) wavelength channels. It is important for these channels to be uncorrelated in order to eliminate any worry about dispersion-induced delay between channels. Figure 22 shows a schematic picture of a WDM transmission system. The concept is quite simple, but reliable implementation can be a considerable challenge.

An attractive feature of WDM is the fact that the only active components of the system remain the optical sources and detectors. The multiplexers/demultiplexers are passive and are therefore intrinsically more reliable than active multiplexers. These schemes range from simple refractive/reflective beam combiners to diffractive approaches and are summarized in Fig. 23. For a multiplexing scheme, the key figure of merit is the insertion loss per channel. A simple 50-50 beam splitter for a two-channel combiner offers simple multiplexing with high insertion loss. If the beam splitter is coated to provide high reflectivity at one wavelength and high transmissivity at the other, the insertion loss is reduced, the coupler becomes wavelength-specific, and the element can act either as a multiplexer or demultiplexer.

Grating combiners offer an effective way to maximize the number of channels while still controlling the insertion loss. The grating shape must be appropriately designed—a problem which is easily solved for a single-wavelength, single-angle geometry. However, the diffraction efficiency is a function both of wavelength and angle of incidence. The optimum combination of a range of wavelengths over a wide angular range will typically

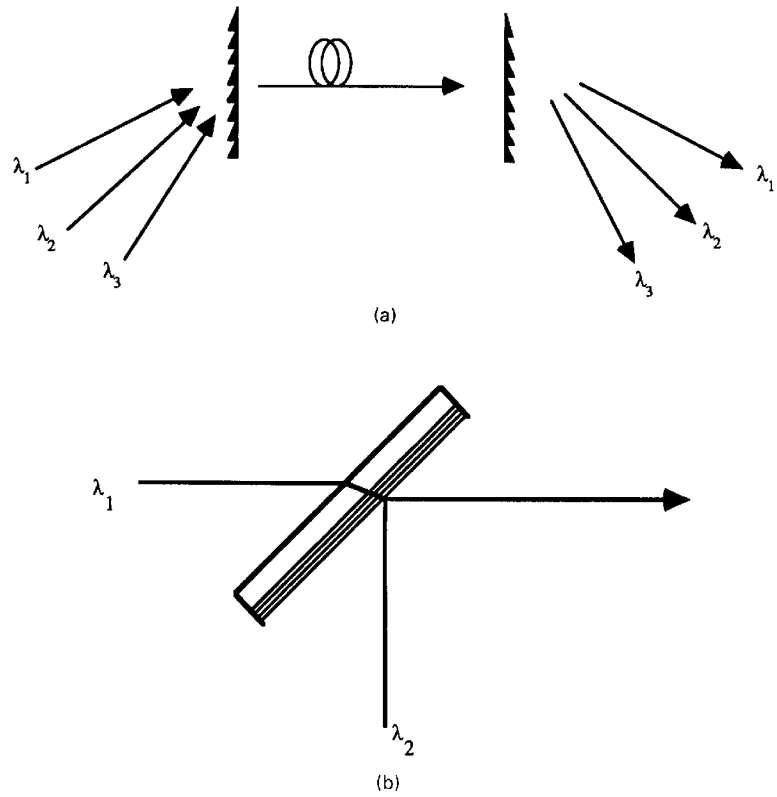

FIGURE 23 Multiplexing/demultiplexing schemes for WDM; (*a*) grating combiner (bulk optics); (*b*) wavelength selective beamsplitter (bulk optics); (*c*) directional coupler (integrated optics); (*d*) all-fiber multiplexer/demultiplexer.

require a tradeoff between insertion loss, wavelength range, and angular discrimination. Wavelength-division multiplexing technology has been greatly aided by the rapid advances in diffractive optics, synthetic holography, and binary optics in recent years. More on these subjects is included in Chap. 8 of Vol. II.

There have been considerable accomplishments in the past ten years in the fabrication of integrated optical components for WDM applications. Much of these involve the waveguide equivalent of bulk diffractive optical elements. Since the optical elements are passive and efficient fiber coupling is required, glass waveguides have often been the medium of choice. A great variety of couplers, beam splitters, and multiplexer/demultiplexers have been successfully fabricated in ion-exchanged glass waveguides. Further details on the properties of these waveguides is contained in Chap. 36 of Vol. I. There has also been a major effort to fabricate low-cost polymer-based WDM components. These can be in the form of either waveguides or fibers.

From the point of view of connectivity and modular design, all-fiber WDM components are the most popular. Evanescent single-mode fiber couplers are inherently wavelength-sensitive and can be designed for minimum insertion loss. As with the bulk approaches, all-fiber components become more difficult to design and optimize as the number of

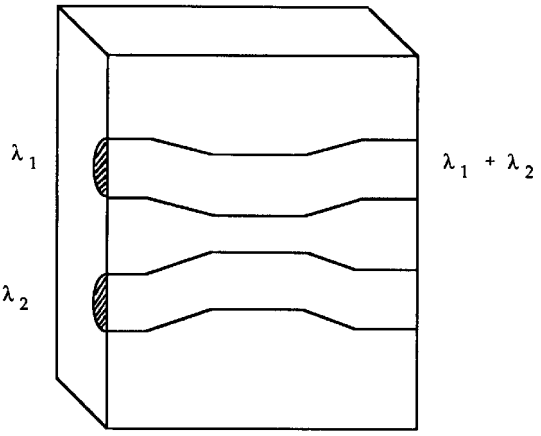

(c)

(d)

FIGURE 23 (*Continued*)

channels increases. Most commercially available all-fiber components are designed for widely separated wavelength channels. For example, Corning, Inc. currently offers multiplexers designed for combining signals from 1.5-μm, 1.3-μm, and 0.8-μm sources.

Advances in source fabrication technology in recent years have offered the possibility of fabricating diode laser arrays equipped with a controlled gradient in emission wavelength across the array. Such an array, equipped with appropriate beam-combining optics, could greatly reduce the packaging and alignment requirements in a large-scale WDM system. Minimizing crosstalk for closely spaced wavelength channels presents a significant challenge for demultiplexer design.

Coherent Optical Communications. Intensity modulation with direct detection remains the most popular scheme for optical communications systems. Under absolutely ideal transmission and detection conditions (no source RIN, perfect photon-counting detection, no background radiation), the probability of detecting n photons in a pulse train having an average of N_P photons per pulse would obey the Poisson distribution

$$p(n) = \frac{N_p^n e^{-N_P}}{n!} \tag{30}$$

The probability of an "error" P_E would be the detection of no photons during the pulse,

$$P_E = \exp(-N_P) \tag{31}$$

If we choose the benchmark error probability of 10^{-9}, we require an average of about 21 photons per pulse. This represents the quantum limit for the direct detection of optical

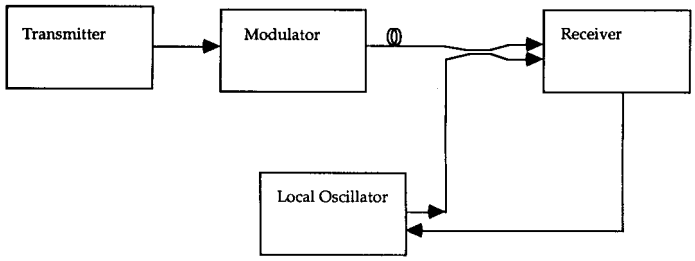

FIGURE 24 Generic coherent optical fiber communication link.

signals. This limit can scarcely be reached, since it assumes no dark count and perfectly efficient photon counting.

Current optical communication[48–54] offers a way to achieve quantum-limited receiver sensitivities even in the presence of receiver noise. By using either amplitude, phase, or frequency modulation combined with heterodyne or homodyne detection, it is possible to approach, and even exceed, the quantum limit for direct detection.

A generic coherent optical communication link is shown in Fig. 24. The crucial differences with direct detection lie in the role of the modulator in transmission and the presence of the local oscillator laser in reception. To understand the role of the modulator, we first consider the method of heterodyne detection. We will then discuss the component requirements for a coherent optical fiber communication link.

Heterodyne and Homodyne Detection. We consider the receiver shown in Fig. 25, in which an optical signal arriving from some distant point is combined with an intense local oscillator laser by use of a 2×2 coupler. The power $I(r)$ guided in the single-mode fiber due to the interfering amplitudes can be expressed as

$$I(r) = P_S(t)\,|\Psi_S(r)|^2 + P_{LO}\,|\Psi_{LO}(r)|^2 + 2e_S(t) \cdot e_{LO}\Psi_S(r)\Psi_{LO}(r)\sqrt{P_S(t)P_{LO}}\cos(\omega_{IF}t + \Delta\phi) \quad (32)$$

in which $e_{LO}(t)$ and $e_S(t)$ denote the polarizations of the local oscillator and signal, P_{LO} and $P_S(t)$ denote the powers of the local oscillator and signal, $\Psi_S(r)$ and $\Psi_{LO}(r)$ are the spatial amplitude distributions, and $\Delta\phi(t)$ denotes the phase difference between the two sources. The two sources may oscillate at two nominally different frequencies, the difference being labeled the *intermediate frequency* ω_{IF} (from heterodyne radio nomenclature). If the

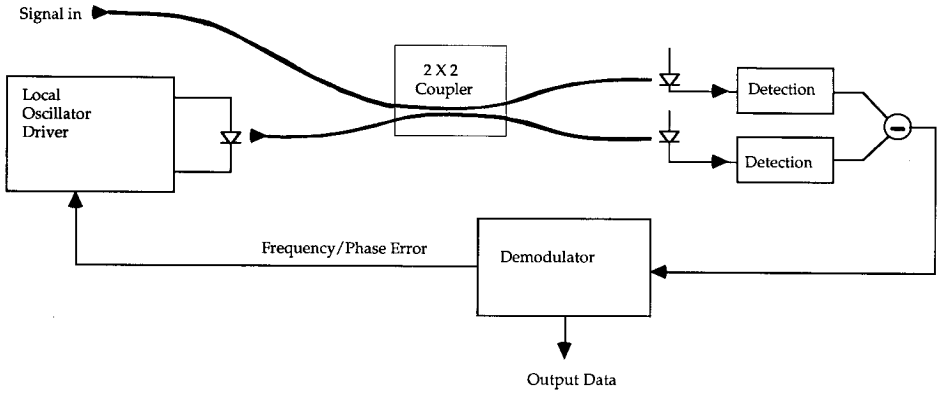

FIGURE 25 Heterodyne/homodyne receiver.

intermediate frequency is zero, the detection process is termed *homodyne* detection; if a microwave or radio carrier frequency is chosen for postdetection processing, the detection process is referred to as *heterodyne* detection.

If the local oscillator power is much larger than the signal power, the first term is negligible. The second represents a large, continuous signal which carries no information but does provide a shot noise contribution. The third term represents the signal information. If the signal is coupled to a detector of responsivity R and ac-coupled to eliminate the local oscillator signal, the photocurrent $i(t)$ can be expressed as follows:

$$i(t) = 2R\eta_{\text{HET}}\sqrt{P_S(t)P_{LO}}\cos(\omega_{IF}t + \Delta\phi) \tag{33}$$

The heterodyne efficiency η_{HET} is determined by the spatial overlap of the fields and the inner product of the polarization components:

$$\eta_{\text{HET}} = (e_S(t) \cdot e_{LO}) \int_{\substack{\text{Fiber}\\ \text{Area}}} \Psi_S(r)\Psi_{LO}(r)\, d^2r \tag{34}$$

These results illustrate four principles of coherent optical fiber communications:

1. The optical frequency and phase of the signal relative to those of the local oscillator are preserved, including the phase and frequency fluctuations.

2. The local oscillator "preamplifies" the signal, yielding a larger information-carrying component of the photocurrent than would be detected directly.

3. The local oscillator and signal fields must occupy the same spatial modes. Modes orthogonal to that of the local oscillator are rejected.

4. Only matching polarization components contribute to the detection process.

The first principle allows the detection of frequency or phase information, provided the local oscillator has sufficient stability. The second provides an improvement of the signal-to-noise ratio in the limit of large local oscillator power. Both the first and fourth lead to component requirements which are rather more stringent than those encountered with direct detection. The following sections will discuss the source, modulator, fiber, and receiver requirements in a coherent transmission system.

Receiver Sensitivity. Let σ_T^2 represent the receiver noise described in Eq. 26. The signal-to-noise ratio for heterodyne detection may be expressed as

$$\text{SNR} = \frac{2\eta_{\text{HET}}R^2P_SP_{LO}}{2eRP_{LO}B_n + \sigma_T^2} \tag{35}$$

where B_n denotes the noise bandwidth of the receiver. (B_n is generally about half of the data rate for digital systems.) For homodyne detection, the signal envelope carries twice the energy, and

$$\text{SNR} = \frac{4\eta_{\text{HET}}R^2P_SP_{LO}}{2eRP_{LO}B_n + \sigma_T^2} \tag{36}$$

For a given modulation scheme, homodyne detection will therefore be twice as sensitive as heterodyne.

Modulation Formats. The modulation formats appropriate for coherent optical communications can be summarized as follows:

1. *Amplitude-Shift Keying (ASK).* This technique is simply on-off keying (similar to simple intensity modulation) but with the important constraint that the frequency and phase of the laser be kept constant. Direct modulation of ordinary semiconductor lasers produces a frequency chirp which is unacceptable for ASK modulation. An external

modulator such as an electro-optic modulator, a Mach-Zehnder modulator, or an electroabsorption modulator would therefore be appropriate for ASK.

2. *Phase-Shift Keying* (*PSK*). This technique requires switching the phase between two or more values. Any phase modulator can be suitable for phase-shift keying. Direct modulation of semiconductor lasers is not suitable for PSK for the same reasons mentioned for ASK.

3. *Frequency-Shift Keying* (*FSK*). FSK has received a good deal of attention[55] because it can be achieved by direct modulation of the source. It is possible to make use of the natural frequency chirp of the semiconductor laser to frequency modulate the laser simply by a small modulation of the drive current.

All of the modulation techniques can operate between two states (binary) or extend to four or more levels. The only technique which benefits from an increase in the number of channels is FSK. The sensitivity of PSK to source phase noise generally precludes higher-level signaling. Multilevel FSK, being a bandwidth expansion technique, offers a receiver sensitivity improvement over binary FSK without placing severe constraints on the source.

Table 4 gives expressions for the receiver error probability as a function of received power for each modulation technique. The right-hand column gives, for comparison purposes, the number of photons required per pulse to assure an error rate of better than 10^{-9}. PSK modulation with homodyne detection is the most sensitive, requiring only nine photons per pulse, which is below the quantum limit for direct detection.

Source Requirements. One of the ways coherent optical communications systems differ from their microwave counterparts is in the comparatively large phase noise of the source. Since the detection system is sensitive to the frequency and phase of the laser, the source linewidth is a major consideration. This is very different from intensity modulation/direct detection, in which the source spectral width limits the system only through the channel dispersion. When two sources are heterodyned to generate an intermediate frequency in the microwave region, the spectral spread of the heterodyned signal is the combined spectral spread of the signal and local oscillator. Thus, the rule of thumb for high-quality coherent detection is that the sum of the linewidths of the signal and local oscillator be much less than the receiver bandwidth.

TABLE 4 Receiver Sensitivities for a Variety of Modulation/Detection Schemes

Modulation/Detection Scheme	P_E	Photons per pulse @ $P_E = 10^{-9}$
ASK heterodyne	$0.5erfc\left(\sqrt{\frac{\eta P_S}{4h\nu B}}\right)$	72
ASK homodyne	$0.5erfc\left(\sqrt{\frac{\eta P_S}{2h\nu B}}\right)$	36
FSK heterodyne	$0.5erfc\left(\sqrt{\frac{\eta P_S}{2h\nu B}}\right)$	36
PSK heterodyne	$0.5erfc\left(\sqrt{\frac{\eta P_S}{h\nu B}}\right)$	18
PSK homodyne	$0.5erfc\left(\sqrt{\frac{2\eta P_S}{h\nu B}}\right)$	9
Direction detection quantum limit	$0.5\exp\left(\frac{-\eta P_S}{h\nu B}\right)$	21

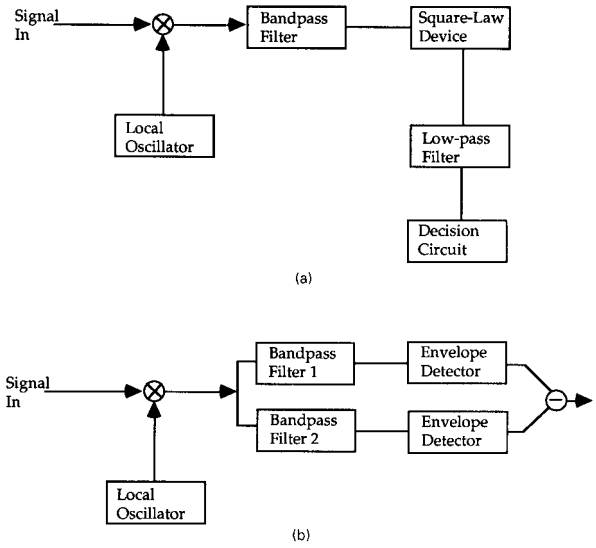

FIGURE 26 Noncoherent (asynchronous) demodulation schemes: (*a*) ASK envelope detection; (*b*) FSK dual filter detection, in which the signal is separated into complementary channels for ASK envelope detection.

Precisely how narrow the linewidth must be has been a topic of many papers.[49–52] The result varies somewhat with modulation scheme and varies strongly with the demodulation process. The general trends can be summarized as follows:

Incoherent demodulation (envelope detection). Either ASK or FSK can be demodulated simply by using an appropriate combination of filters and nonlinear elements. The basic principle of incoherent ASK or dual-filter FSK detection is illustrated in Fig. 26. This type of detection is, in general, least sensitive to the spectral width of the source. The primary effect of a broad source is to broaden the *IF* signal spectrum, resulting in attenuation but not a catastrophic increase in bit error rate. Further, the receiver bandwidth can always be broadened to accommodate the signal. This yields a penalty in excess receiver noise, but the source spectral width can be a substantial fraction of the bit rate and still keep the receiver sensitivity within tolerable limits.

There are two approaches to PSK detection which avoid the need for a phase-locked loop. The first is differential phase-shift keying (DPSK), in which the information is transmitted in the form of phase *differences* between neighboring time slots. The second is phase diversity reception, in which a multiport interferometer is designed to yield signals proportional to the power in different phase quadrants.

Coherent demodulation with electronic phase-locked loop. Some PSK signals cannot be demodulated incoherently and require careful receiver design for proper carrier recovery. Suppressed carrier communications schemes such as PSK require a nonlinear recovery circuit. The phase estimation required in proper carrier recovery is far more sensitive to phase noise than is the case with envelope detection. In contrast to incoherent demodulation, source spectral widths must generally be kept to less than 1 percent of the bit rate (10 percent of the phase-locked loop bandwidth) to maintain reliable detection.

Coherent demodulation with optoelectronic phase-locked loop. Homodyne detection requires that an error signal be fed back to the local oscillator; phase and frequency errors must be corrected optically in order to maintain precise frequency and phase matching between the two signals. This generally results in a narrower phase-locked loop bandwidth

and a much narrower spectral width requirement for the transmitter and local oscillator. Homodyne systems therefore require considerably narrower linewidths than their heterodyne counterparts.

Fiber Requirements. Heterodyne or homodyne reception is inherently single-mode, and it is therefore necessary for coherent links to use single-mode fibers. Single-mode couplers can then be used to combine the signal and local oscillator lasers for efficient heterodyne detection.

As with other forms of fiber communications, fiber dispersion presents a degradation in the signal-to-noise ratio due to differential delay between different components of the signal spectrum. The power penalty associated with fiber dispersion is determined entirely by the dispersion, the fiber length, and the bit rate. Because of the stringent source linewidth requirements for coherent detection, the spectral broadening is entirely due to the signal itself. The coherent detection system is therefore inherently less sensitive to fiber dispersion.

One important requirement of any fiber that is to be used for coherent transmission is polarization control. As was discussed briefly under ''Polarization Characteristics of Fibers'' earlier in this chapter, the transmitted polarization of light from a single-mode fiber varies randomly with temperature, stress on the fiber, and other environmental influences. If heterodyning is attempted under these circumstances, the heat signal will fade in and out as the polarization of the signal changes.

Polarization fading can be controlled either by external compensation,[56] internal control,[11] or polarization diversity reception.[57] External compensation seeks to actively control the polarization of the output by sensing the error through a polarizer-analyzer combination and feeding back to correct the polarization. The latter can be accomplished through mechanical, electro-optical, or magneto-optical means.

There are classes of optical fiber sensors which have source and fiber requirements very similar to those of a coherent communication link. One of the most widely studied has been the optical fiber gyro, in which counterpropagating waves in a rotating fiber coil interfere with one another; the resulting beat frequency between the waves is proportional to the angular velocity of the coil. There are other interferometric sensors which make use of optical fibers. Most of them require polarization control and a high degree of frequency stability for the source. The relatively low frequencies and small bandwidths which are required for sensing represent the major difference between these applications and coherent data transmission.

10.8 NONLINEAR OPTICAL PROPERTIES OF FIBERS

Chapters and entire books have been devoted to the subject of optical nonlinearities in fibers. A selection of these are included in ''Further Reading'' at the end of this chapter. We will content ourselves with an overview of the subject, and consider nonlinear effects which are most important in either limiting or enhancing the performance of fibers. To date, most of the *applications* of nonlinear optics in fibers are in the area of ultralong distance telecommunications.[41,58–60] However, nonlinearities can limit the power-handling ability of fibers and can be an important limitation for certain medical/surgical applications.

Stimulated Scattering Processes

The low loss and long interaction length of an optical fiber makes it an ideal medium for stimulating even relatively weak scattering processes. Two important processes in fibers are: (1) stimulated Raman scattering, the interaction of the guided wave with high-frequency optical phonons in the material, and (2) stimulated Brillouin scattering, the

emission, amplification, and scattering of low-frequency acoustic waves. These are distinguished by the size of the frequency shift and the dynamics of the process, but both can act to limit the power available for transmission.

Stimulated Raman scattering (SRS) produces a frequency shift of about 400 cm^{-1} from the incident laser line. The equation governing the power growth of the Raman-shifted mode is as follows

$$\frac{dP_R}{dz} = -\alpha_R P_R + \frac{g_R}{a_P} P_P P_R \tag{37}$$

where P_R denotes the power of the Stokes-shifted light, P_P is the pump power (this is the power in the initially excited mode), and a_P is the effective area of the pump. The Raman gain g_R ultimately determines the SRS-limited light intensity. For typical single-mode silica fibers, g_R is about 10^{-11} cm/W, and yields a power limit of

$$P_{CR} = \frac{16\alpha a_P}{g_R} \tag{38}$$

beyond which the guided wave power will be efficiently Raman-shifted and excess loss will begin to appear at the pump wavelength.

Stimulated Brillouin scattering (SBS) can yield an even lower stimulated scattering threshold. Acoustic waves in the fiber tend to form a Bragg index grating, and scattering occurs primarily in the backward direction. The Brillouin gain g_B is much higher than Raman gain in fibers ($g_B = 5 \times 10^{-9}$ cm/W) and leads to a stimulated scattering threshold of

$$P_{CR} = \frac{25\alpha a_P}{g_B} \tag{39}$$

for a narrowband, CW input.

Either type of stimulated scattering process can be used as a source of gain in the fiber. Injecting a signal within the frequency band of the stimulated scattering process will provide amplification of the input signal. Raman amplification tends to be the more useful of the two because of the relatively large frequency shift and the broader-gain bandwidth. SBS has been used in applications such as coherent optical communications[48] where amplification of a pilot carrier is desired.

The gain bandwidth for SBS is quite narrow—100 MHz for a typical fiber. SBS is therefore only important for sources whose spectra lie within this band. An unmodulated narrow-band laser source such as would be used as a local oscillator in a coherent system would be highly susceptible to SBS, but a directly modulated laser with a 1-GHz linewidth under modulation (modulated laser linewidths can extend well into the GHz range due to frequency chirp) would have an SBS threshold about ten times that of the narrow linewidth source.

Pulse Compression and Soliton Propagation

A major accomplishment in the push toward short pulse propagation in optical fibers was the prediction and observation of solitary wave propagation. In a nonlinear dispersive medium, solitary waves may exist provided the nonlinearity and dispersion act to balance one another. In the case of soliton propagation, the nonlinearity is a refractive index which follows the pulse intensity in a nearly instantaneous fashion:

$$n(t) = n_0 + n_2 I(t) \tag{40}$$

For silica fibers, $n_2 = 3 \times 10^{-16}$ cm^2/W.

TABLE 5 Normalized Variables of the Nonlinear Schrödinger Equation

A	Pulse amplitude
z	Longitudinal coordinate
t	Time
P_0	Peak power
T_0	Pulse width
U	$A/\sqrt{P_0}$ normalized pulse amplitude
β_1	Propagation constant
β_2	Dispersion (2d order)
L_D	$T_0^2/\lvert\beta_2\rvert$ dispersion length
n_2	Nonlinear refractive index
τ	$\dfrac{t-\beta_1 z}{T_0}$ time normalized to moving frame
ξ	$\dfrac{z}{L_D}$ normalized distance
N	$n_2\beta_1 P_0 T_0^2/\lvert\beta_2\rvert$ Order of soliton

The scalar equation governing pulse propagation in such a nonlinear dispersive medium is sometimes termed the *nonlinear Schrödinger equation*

$$i\frac{dU}{d\xi}+\frac{1}{2}\frac{d^2U}{d\tau^2}+N^2|U|^2U=0 \tag{41}$$

where the symbols are defined in Table 5. Certain solutions of this equation exist in which the pulse propagates without change in shape; these are the soliton solutions. Solitons can be excited in fibers and propagate great distances before breaking up. This is the basis for fiber-based soliton communication.

Figure 27 illustrates what happens to a pulse which propagates in such a medium. The local refractive index change produces what is commonly known as *self phase modulation.* Since n_2 is positive, the leading edge of the pulse produces a local increase in refractive index. This results in a red shift in the instantaneous frequency. On the trailing edge, the pulse experiences a blue shift. If the channel is one which exhibits normal dispersion, the red-shifted edge will advance while the blue-shifted edge will retard, resulting in pulse spreading If, however, the fiber exhibits anomalous dispersion (beyond 1.3 μm for most single-mode fibers), the red-shifted edge will retard and the pulse will be compressed. Fibers have been used in this way as pulse compressors for some time. In the normal dispersion regime, the fiber nonlinearity is used to chirp the pulse, and a grating pair supplies the dispersion necessary for compression. In the anomalous dispersion regime, the fiber can act both to chirp and compress the pulse. Near the dispersion minimum,

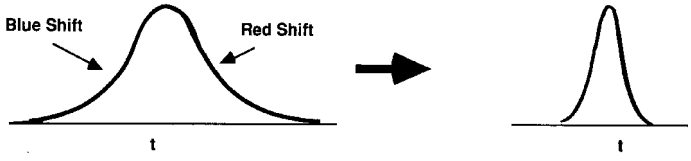

FIGURE 27 A pulse propagating through a medium with an intensity-dependent refractive index will experience frequency shifts of the leading and trailing edges of the pulse (*left*). Upon transmission through a fiber having anomalous dispersion, the pulse compresses (*right*).

higher-order dependence of the group delay on wavelength becomes important, and simple pulse compression does not take place.

Pulse compression cannot continue indefinitely, since the linear dispersion will always act to spread the pulse. At a critical shape, the pulse stabilizes and will propagate without change in shape. This is the point at which a soliton forms. The lowest-order soliton will propagate entirely without change in shape, higher order solitons (which also carry higher energy) experience a periodic evolution of pulse shape.

A soliton requires a certain power level in order to maintain the necessary index change. Distortion-free pulses will therefore propagate only until the fiber loss depletes the energy. Since solitons cannot persist in a lossy channel, they were long treated merely as laboratory curiosities. This was changed by several successful demonstrations of extremely long distance soliton transmission by the inclusion of gain to balance the loss. The gain sections, which initially made use of stimulated Raman scattering, now consist of rare-earth doped fiber amplifiers. The record for repeaterless soliton transmission is constantly being challenged. At the time of this writing, distance of well over 10,000 km have been demonstrated in recirculating loop experiments.

In the laboratory, solitons have most often been generated by mode-locked laser sources. Mode-locked solid state laser sources are generally limited to low duty-cycle pulses, with repetition rates in the 1-GHz range or less. The mode-locked pulse train must then be modulated to carry data, a process which must be carried out externally. There is a high level of current interest in Erbium-doped fiber lasers as mode-locked sources for ultralong distance data communications. Despite the capability of high duty cycle, directly modulated semiconductor lasers are generally rendered unsuitable for soliton communications by the spectral broadening that occurs under modulation.

Four-Wave Mixing

The nonlinear refractive index is simply a degenerate case of a third-order optical nonlinearity, in which the polarization of the medium responds to the cube of the applied electric field. It is possible for widely separated frequencies to phase modulate one another via the fiber nonlinearity, generating sidebands which interfere with neighboring channels in a multiplexed system. This represents an important limit to channel capacity in either WDM or FDM systems. The simplest picture of the four-wave mixing process in fibers can be illustrated by the transmission and cross-phase modulation of four equally spaced channels shown in Fig. 28. Channels 1 and 2 interfere, producing an index of refraction which oscillates at the difference frequency. This modulation in refractive index modulates channel 4, producing sidebands at channels 3 and 5. This is only the simplest combination of frequencies. Four-wave mixing allows any combination of three frequencies beating together to produce a fourth. If the fourth frequency lies within a communication band, that channel can be rendered unusable.

This channel interference can effect either closely spaced channels, as one encounters

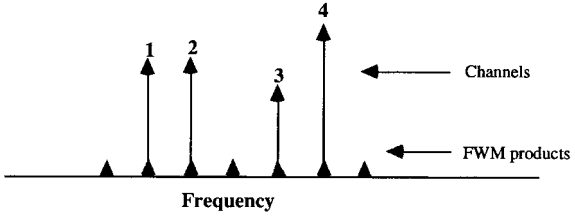

FIGURE 28 The effects of four-wave mixing on multichannel transmission through an optical fiber.

with coherent communications, or the rather widely separated channels of a WDM system. Efficient four-wave mixing requires phase matching of the interacting waves throughout the interaction length—widely separated channels will therefore be phase matched only in a region of low-fiber dispersion.

The communications engineer will recognize this as little more than the intermodulation products which must always be dealt with in a multichannel communications system with small nonlinearities. Four-wave mixing merely produces intermodulation products over an extremely wide bandwidth. Just as with baseband nonlinearities in analog communications systems, judicious allocation of channels can minimize the problem, but at the expense of bandwidth. The cumulative effect of the nonlinearities increases with interaction length and therefore imposes an important limit on frequency or wavelength-division multiplexed systems.

Photorefractive Nonlinearities in Fibers

There also exists a class of integrating, photorefractive nonlinearities in optical fibers which have been of some interest in recent years. We use the word photorefractive loosely here, simply to indicate a long-term change in either the first- or second-order susceptibility with light exposure. The effects appear strongest in fibers with a germania content, but the precise role of the glass constituents in these processes is still an area of active research.

Bragg Index Gratings. Photons of energy near a UV absorption edge can often write permanent phase gratings by photoionizing certain constituents or impurities in the material. This is the case for $LiNbO_4$ and certain other ferroelectric materials, and such effects have also been observed in germania-silica fibers. The effects were first observed in the process of guiding relatively high power densities of green light—it was found that a high backscatter developed over a period of prolonged exposure. The fiber then exhibited the transmission characteristics of a Bragg grating, with extremely high resonant reflectivities.

The writing of permanent gratings in fibers using UV exposure is now relatively commonplace. Bragg gratings can be used as filters in WDM systems, reflectors on fiber lasers, and possibly optical switches. For short lengths, the gratings are most easily formed holographically, by using two interfering beams from a pulsed UV source such as an excimer laser. The fiber is exposed from the side; by controlling the angle of the two interfering beams, any grating period may be chosen.

Frequency Doubling in Germania-Silica Fibers. While it is not surprising that UV exposure could produce refractive index changes, a rather unexpected discovery was the fact that strong optical fields inside the fiber could produce a second-order susceptibility, resulting in efficient frequency doubling. Electro-optic effects such as frequency doubling require that a crystalline material lack a center of symmetry while an amorphous material must lack a statistical center of symmetry. It has long been known that certain materials will develop an electro-optic effect under a suitable applied field. This process, known as *poling,* provides the necessary microscopic alignment of dipoles for development of the nonlinear susceptibility. In optical fibers, a type of self-poling occurs from the strong fundamental beam, resulting in a second-order susceptibility and efficient frequency doubling.

Efficient frequency doubling requires both a noncentrosymmetric material and adequate phase matching between the fundamental and second harmonic waves. The mechanism by which the fiber is both poled and phase matched is still not fully understood at the time of this writing, and it remains to be seen whether this represents an exciting, new application of germania-silica fibers or simply an internal damage mechanism which limits the ultimate power delivery of the fiber.

10.9 OPTICAL FIBER MATERIALS: CHEMISTRY AND FABRICATION

What is arguably the most important breakthrough in the history of optical fiber technology occurred in the materials development. Until 1970, many scientists felt that glasses of moderate softening points and smooth phase transitions would allow for easier drawing and better control. The choice of Corning Glass Works (now Corning, Inc.) to go to (what was then) the somewhat more difficult chemistry of the nearly pure silica fiber allowed both a dramatic reduction in fiber attenuation and a better understanding of the role of the chemical constituents in fiber loss. Researchers soon found that the best dopants for altering the refractive index were those which provided a weak index change without providing a large shift in the UV absorption edge. Conventional fiber chemistry consists of dopants such as GeO_2, P_2O_5 (for raising the refractive index) and B_2O_3 or SiF_4 (for lowering the refractive index).

Silica has both UV and mid-IR absorption bands; these two bands result in a fundamental limit to the attenuation which one can achieve in the silica system. This occurs despite the fact that the Rayleigh scattering contribution decreases as λ^{-4}, and the ultraviolet Urbach absorption edge decreases even faster with increasing λ. The infrared absorption increases with long wavelengths, and becomes dominant beyond wavelengths of about 1.6 μm, resulting in a fundamental loss minimum near 1.55 μm.

The promise of achieving a lower Rayleigh scattering limit in the mid-infrared (as well as the possible applications of fiber to the CO_2 laser wavelength range) have spurred a great deal of research in fiber materials which exhibit better infrared transparency. Two important representative materials are the heavy-metal fluoride glasses and the chalcogenide glasses. While both classes exhibit better infrared transparency, neither has yet improved to the point of serious competition with silica materials.

For a number of years, attenuation in optical fibers was limited by a strong absorption band near $\lambda = 1.4$ μm. (An examination of attenuation curves of early telecommunications-grade fiber shows it nearly unusable at what are now the wavelengths of prime interest—1.3 μm and 1.55 μm.) This absorption, which was linked to the presence of residual OH ions, grew steadily lower with the improvement of fiber fabrication techniques until the loss minimum at $\lambda = 1.55$ μm was eventually brought close to the Rayleigh scattering limit.

The low-cost, low-temperature processes by which polymers can be fabricated has led to continued research into the applications of plastic fiber to technologies which require low cost, easy connectivity, and that are not loss-limited. The additional flexibility of these materials makes them attractive for large-core, short-length applications in which one wishes to maximize the light insertion. Hybrid polymer cladding-silica core fibers have also received some attention in applications requiring additional flexibility.

The final triumph of fiber chemistry in recent years has been the introduction and successful demonstration of extremely long distance repeaterless fiber links using rare-earth doped fiber amplifiers. This represented the climax of a long period of research in rare-earth doped glasses which went largely unnoticed by the optics community. As a result, there has been an explosion of work in the materials science, materials engineering, and applications of rare-earth doped optical fibers.

Fabrication of Conventional Optical Fibers

Conventional fabrication of low-loss optical fibers requires two stages. The desired refractive index profile is first fabricated in macroscopic dimensions in a preform. A typical preform is several centimeters in width and a meter in length, maintaining the dimensions and dopant distribution in the core and cladding that will eventually form in the fiber.

Chemical vapor deposition (CVD) is the primary technology used in fiber manufacturing. The fabrication process must satisfy two requirements: (1) high purity, and (2) precise control over composition (hence, refractive index) profiles. Manufacturing considerations favor approaches which provide a fast deposition rate and comparatively large preforms. In CVD processes, submicron silica particles are produced through one (or both) of the following chemical reactions

$$SiCl_4 + O_2 \rightarrow SiO_2 + 2Cl_2$$

$$SiCl_4 + 2H_2O \rightarrow SiO_2 + HCl$$

The reactions are carried out at a temperature of about 1800°C. The deposition leads to a high-purity silica soot which must then be sintered in order to form optical quality glass.

Modern manufacturing techniques, generally speaking, use one of two processes.[61] In the so-called ''inside process,'' a rotating silica substrate tube is subjected to an internal flow of reactive gases. The two inside processes which have received the most attention are modified chemical vapor deposition (MCVD) and plasma-assisted chemical vapor deposition (PCVD). Both techniques require a layer-by-layer deposition, controlling the composition at each step in order to reach the correct target refractive index. Oxygen, as a carrier gas, is bubbled through $SiCl_4$, which has a relatively high vapor pressure at room temperature.

The PCVD process provides the necessary energy for the chemical reaction by direct RF plasma excitation. The submicron-sized particles form on the inner layer of the substrate, and the composition of the layer is controlled strictly by the composition of the gas. PCVD does not require the careful thermal control of other methods, but requires a separate sintering step to provide a pore-free preform. A final heating to 2150°C collapses the preform into a state in which it is ready to be drawn.

The MCVD process (Fig. 29) accomplishes the deposition by an external, local application of a torch. The torch has the dual role of providing the necessary energy for oxidation and the heat necessary for sintering the deposited SiO_2. The submicron particles are deposited on the ''leading edge'' of the torch; as the torch moves over these particles, they are sintered into a vitreous, pore-free layer. Multiple passes result in a layered, glassy deposit which should approximate the target radial profile of the fiber. As with PCVD, a final pass is necessary for collapse of the preform before the fiber is ready to be drawn. MCVD requires rather precise control over the temperature gradients in the tube but has the advantage of accomplishing the deposition and sintering in a single step.

In the ''outside process,'' a rotating, thin cylindrical target (or mandrel) is used as the substrate for a subsequent chemical vapor deposition, and requires removal before the

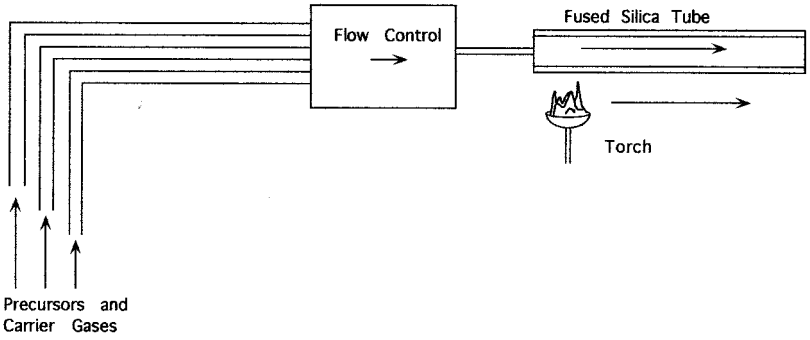

FIGURE 29 The modified chemical vapor deposition (MCVD) process for preform fabrication.

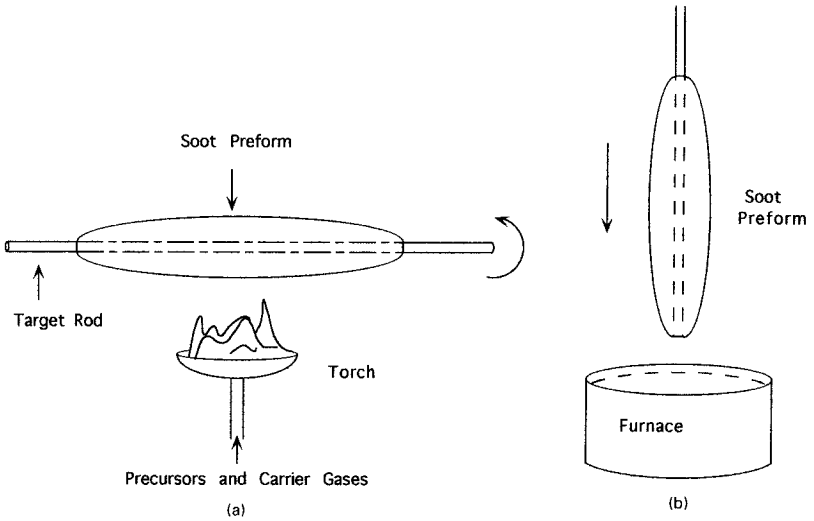

FIGURE 30 Outside method of preform fabrication. The soot deposition (*a*) is followed by sintering (*b*) to cast the preform.

boule is sintered. Much of the control in these deposition techniques lies in the construction of the torch. For an outside process, the torch supplies both the chemical constituents and the heat for the reaction.

Two outside processes which have been used a great deal are the outside vapor deposition (OVD) and the vapor axial deposition (VAD) techniques. Figure 30 illustrates a generic outside process. In the OVD process the torch consists of discrete holes formed in a pattern of concentric rings. The primary chemical stream is at the center, followed by O_2 (acting as a shield gas), premixed methane/oxygen, and another shield ring. The torch itself translates along the rotating boule and the dopants are dynamically controlled to achieve the necessary profiling.

The VAD torch is comprised of a set of concentric annular apertures, with a chemical sequence similar to the OVD. In contrast to the OVD method, the VAD torch is held stationary during the deposition; the rotating target is held vertically, and is lifted as the deposition continues.

Dopant Chemistry

Standard dopants for silica fiber include GeO_2, P_2O_5, B_2O_3, and SiF_4. The former two are used to increase the refractive index (and are therefore used in the core), while the latter decrease the index of refraction (and are therefore used in the cladding). The CVD processes will often use oxygen as a carrier gas with the high vapor pressure liquids $GeCl_4$, $POCl_3$, or SiF_4. The reaction which produces the dopant ''soot'' is then

$$GECl_4 + O_2 \rightarrow GeO_2 + 2Cl_2$$

$$4POCl_3 + 3O_2 \rightarrow 2P_2O_5 + 6Cl_2$$

As noted in a recent article by Morse et al.,[62] ''Nature has been kind in the creation of the high vapor pressure liquid precursors used in the fabrication of optical fibers for the transmission of telecommunication signals.'' This has been an extremely important factor

in the success of CVD fiber fabrication techniques. The problem of introducing more exotic dopants, such as the rare-earth elements, is not quite so straightforward and there does not appear to exist, at this time, a single, widely used technique. The problem of control over the rare-earth dopant profile is compounded by the fact that research in laser and amplifier design is ongoing, and the optimum dopant profile for rare-earth doped fibers and amplifiers is, in many cases, still unknown. Despite these uncertainties, rare-earth doped fibers have already been introduced into commercial products and promise to spearhead the next generation of long distance telecommunications systems.

Other Fabrication Techniques

There are other preform fabrication and fiber drawing techniques. These are not generally used in telecommunications-grade silica fiber, but can be of advantage for glass chemistries which do not easily lend themselves to chemical vapor deposition. Several examples of this will be described in the following section on infrared fiber fabrication.

CVD materials, while the most popular, are not the only methods for preform fabrication. Alternative methods of preform fabrication include both bulk casting and a class of non-CVD tubular casting techniques. One such technique is the ''rod-in-tube'' method, in which the core and cladding materials are cast separately and combined in a final melting/collapsing step. This method assures a homogeneous, low-impurity content core but risks introducing defects and bubbles into the core/cladding interface.

The most well-known method of *preform-free drawing* is the double crucible method, in which the core and cladding melts are formed separately and combined in the drawing process itself. This eliminates the need for a very large preform in the case of long lengths of fiber. The index profile is established in the drawing process itself, and index gradients are therefore difficult to establish unless additional crucibles are added. Another difficulty of the crucible method is the sometimes inadequate control of the concentricity of the core and cladding.

Infrared Fiber Fabrication

The major applications of interest for infrared optical fibers are as follows:

1. Ultra-low-loss communication links
2. CO_2 laser transmission for medical applications
3. Thermal imaging and remote temperature monitoring
4. Gas sensing

These may differ rather dramatically in their attenuation requirements and spectral region of interest. For example, an ultra-low-loss communications link requires attenuation somewhat less than 0.1 dB/km in order to be competitive with silica fiber. Typical medical applications simply require high-power handling capabilities of a CO_2 laser over meter lengths. All of these applications require a departure from the silica-based chemistry which has been so successful for applications in the near infrared and visible. Much of the generic chemistry of these glasses is covered in Chap. 33 of Vol. II, ''Crystals and glasses''. Our intent here is to give an overview of the fiber types and the general state of the materials technology in each case.

Chalcogenide Fibers. Sulfide, selenide, and telluride glasses have all been used for bulk infrared optics—particularly for applications involving CO_2 ($\lambda = 10.6\ \mu m$) or CO laser transmission ($\lambda = 5.4\ \mu m$). Infrared fibers have been drawn from these materials and

yielded transmission losses of the order of 1 dB/meter in the 5- to 7-μm region.[63] The preform fabrication and drawing of chalcogenide fibers is much more difficult than that of silica due primarily to its sensitivity both to oxygen and moisture. Both oxidation and crystallization can occur at the temperatures necessary to draw the fiber. Either will result in catastrophically high losses and fiber weakness.

Fluoride Fibers. Fluoride fibers have received the most attention for low-loss telecommunications applications, because the theoretical limit for Rayleigh scattering is considerably lower. This is due both to a higher-energy UV absorption edge and better infrared transparency. The difficulty is that excess absorption has proven rather difficult to reduce, and the lowest published losses to date have been near 1 dB/km for long fiber lengths.[64,65] The state-of-the-art in fluoride fiber fabrication is still well above the Rayleigh scattering limit but does show the expected improvement over silica fiber in wavelengths beyond 1.6 μm. Fabrication of very short fiber lengths has been somewhat more successful, with reported losses as low as 0.025 dB/km at 2.55 μm.[66]

The residual loss for longer fibers has been largely linked to extrinsic impurity/defect content. Recent articles by Takahashi and Sanghera[64,65] have noted the role of transition metal and rare-earth ions, submicron platinum particles, oxyfluoride particles, fluoride microcrystals, and bubbles as both extrinsic absorbers and scatterers. The defects of interest originate from a variety of sources, and there has been much discussion on which defects dominate the scattering process. To date, the consensus appears to be that impurity absorption does *not* adequately account for the current loss limits, but does account for residual losses in the neighborhood of 0.2 dB/km.

The classes of defects which have been blamed for the current loss limits are as follows:

Platinum particles. These arise from the use of platinum crucibles. The use of vitreous carbon crucibles eases this contamination.

Core bubbles. This is clearly a problem in the preform fabrication and appears in some of the bulk casting techniques.

Interfacial bubbles. Bubbles appearing at the core-cladding interface have been named as being a major cause of excess scattering. These appear to be a particular problem for those techniques which employ separate core and cladding melts. This unfortunately negates some of the advantages offered by the crucible techniques in fluoride fiber fabrication.

Fluoride microcrystals. Crystals can nucleate at a variety of defect sites. Many of these sites appear at the core-cladding interface, producing interface roughness and scattering. Since, for step-index fibers, the integrity of the core-cladding interface is essential to the confinement of the optical wave, a small amount of interface roughness can produce rather high excess losses.

Chapter 33 of Vol. II, ''Crystals and glasses'', gives information on the composition and properties of a single-mode fiber grade fluoride glass. This class of compositions has received the designation ZBLAN, after its heavy-metal constituents. The large number of components makes it immediately obvious that both phase separation and crystallization are important issues in fabrication. Either can produce catastrophic increases in loss as well as mechanical weakening of the fiber, and it is clear that many materials science challenges remain in the area of fluoride fiber fabrication.

10.10 REFERENCES

1. K. C. Kao and G. A. Hockham, ''Dielectric Fibre Surface Waveguides for Optical Frequencies'', *Proc. IEE,* **113,** 1966, pp. 1151–1158.
2. D. B. Keck, P. C. Schultz, and F. W. Zimar, U.S. Patent 3,737,393.

3. F. P. Kapron, D. B. Keck, and R. D. Maurer, ''Radiation Losses in Glass Optical Waveguides'' *Appl. Phys. Lett.,* **17,** 1970, p. 423.
4. M. J. Adams, *An Introduction to Optical Waveguides,* John Wiley and Sons, Chichester, 1981.
5. D. Davidson, ''Single-Mode Wave Propagation in Cylindrical Optical Fibers'', in E. E. Basch (ed.), *Optical Fiber Transmission,* Howard W. Sams, Indianapolis, 1987, pp. 27–64.
6. M. O. Vassell, ''Calculation of Propagating Modes in a Graded-Index Optical Fiber'', *Optoelectronics,* **6,** 1974, pp. 271–286.
7. D. Gloge, ''Weakly Guiding Fibers'', *Appl. Opt.,* **10,** 1971, pp. 2252–2258.
8. R. W. Davies, D. Davidson, and M. P. Singh, ''Single Mode Optical Fiber with Arbitrary Refractive Index Profile: Propagation Solution by the Numerov Method'', *J. Lightwave Tech.,* LT-3, 1985, pp. 619–627.
9. P. C. Chow, ''Computer Solutions to the Schroedinger Problem'', *Am. J. of Physics,* **40,** 1972, pp. 730–734.
10. A. Kumar, R. K. Varshney, and K. Thyagarajan, ''Birefringence Calculations in Elliptical-core Optical Fibers'', *Electron. Lett.,* **20,** 1984, pp. 112–113.
11. K. Sano and Y. Fuji, ''Polarization Transmission Characteristics of Optical Fibers With Elliptical Cross Section'', *Electron. Commun. Japan,* **63,** 1980, p. 87.
12. EIA-FOTP-46, *Spectral Attenuation Measurement for Long-Length, Graded-Index Optical Fibers, Procedure B,* Electronic Industries Association (Washington, D.C.).
13. EIA-FOTP-78, *Spectral Attenuation Cutback Measurement for Single Mode Optical Fibers*, Electronic Industries Association (Washington, D.C.).
14. EIA-FOTP-50, *Light Launch Conditions for Long-Length, Graded-Index Optical Fiber Spectral Attenuation Measurements, Procedure B,* Electronic Industries Association (Washington, D.C.).
15. A. W. Carlisle, ''Small Size High-performance Lightguide Connector for LAN's, *Proc. Opt. Fiber Comm.,* 1985, paper TUQ 18, p. 74–75.
16. E. Sugita, et al., ''SC-Type Single-Mode Optical Fiber Connectors'', *J. Lightwave Tech.,* **LT-7,** 1989, pp. 1689–1696.
17. N. Suzuki, M. Saruwatari, and M. Okuyama, ''Low Insertion- and High Return-loss Optical Connectors with Spherically Convex-polished Ends.'' *Electron. Lett.,* **22**(2)**,** 1986, pp. 110–112.
18. W. C. Young, et al., ''Design and Performance of the Biconic Connector Used in the FT3 Lightwave System,'' in *30th IWCS,* 1981.
19. EIA-FOTP-168, *Chromatic Dispersion Measurement of Multimode Graded-Index and Single-Mode Optical Fibers by Spectral Group Delay Measurement in the Time Domain,* Electronic Industries Association (Washington, D.C.).
20. R. Rao, ''Field Dispersion Measurement—A Swept-Frequency Technique,'' in *NBS Special Publication 683,* Boulder, 1984, p. 135.
21. L. G. Cohen and J. Stone, ''Interferometric Measurements of Minimum Dispersion Spectra in Short Lengths of Single-Mode Fiber,'' *Electron. Lett.,* **18,** 1982, p. 564.
22. L. G. Cohen, et al., ''Experimental Technique for Evaluation of Fiber Transmission Loss and Dispersion,'' *Proc. IEEE,* **68,** 1980, p. 1203.
23. R. A. Modavis and W. F. Love, ''Multiple-Wavelength System for Characterization of Dispersion in Single-Mode Optical Fibers'', in *NBS Special Publication 683,* Boulder, 1984, p. 115.
24. T. Miya, et al., ''Fabrication of Low-dispersion Single-Mode Fiber Over a Wide Spectral Range'', *IEEE J. Quantum Electronics,* **QE-17,** 1981, p. 858.
25. R. Olshansky and R. D. Maurer, ''Tensile Strength and Fatigue of Optical Fibers'', *J. Applied Physics,* **47,** 1976, pp. 4497–4499.
26. EIA-FOTP-28, *Method for Measuring Dynamic Tensile Strength of Optical Fibers,* Electronic Industries Association (Washington, D.C.).
27. M. R. Brininstool, ''Measuring Longitudinal Strain in Optical Fibers,'' *Optical Engineering,* **26,** 1987, p. 1113.
28. M. J. Matthewson, C. R. Kurkjian, and S. T. Gulati, ''Strength Measurement of Optical Fibers by Bending,'' *J. Am. Ceramic. Soc.,* **69,** 1986, p. 815.

29. W. Weibull, ''A Statistical Distribution Function of Wide Applicability,'' *J. Appl. Mech.,* **24,** 1951, pp. 293–297.
30. J. D. Helfinstine, ''Adding Static and Dynamic Fatigue Effects Directly to the Weibull Distribution,'' *J. Am. Ceramic Soc.,* **63,** 1980, p. 113.
31. D. Inniss, D. L. Brownlow, and C. R. Kurkjian, ''Effect of Sodium Chloride Solutions on the Strength and Fatigue of Bare Silica Fibers,'' *J. Am. Ceramic Soc.,* **75,** 1992, p. 364.
32. J. S. Cook and O. I. Scentesi, ''North American Field Trials and Early Applications in Telephony,'' *IEEE J. Selected Areas in Communications,* **SAC-1,** 1983, pp. 393–397.
33. H. Ishio ''Japanese Field Trials and Early Applications in Telephony.'' *IEEE J. Selected Areas in Communications,* **SAC-1,** 1983, pp. 398–403.
34. A. Moncolvo and F. Tosco, ''European Field Trials and Early Applications in Telephony'', *IEEE J. Selected Areas in Communications,* **SAC-1,** 1983, pp. 398–403.
35. E. E. Basch, R. A. Beaudette, and H. A. Carnes, ''Optical Transmission for Interoffice Trunks,'' *IEEE Trans. on Communications,* **COM-26,** 1978, pp. 1007–1014.
36. G. P. Agrawal, *Fiber-Optic Communication Systems,* Wiley Series in Microwave and Optical Engineering, K. Chang (ed.), John Wiley and Sons, New York, 1992.
37. K. Petermann, *Laser Diode Modulation and Noise,* Kluwer Academic, Dordrecht, The Netherlands, 1991.
38. R. J. McIntyre, ''Multiplication Noise in Uniform Avalanche Diodes,'' *IEEE Trans. Electron Devices,* **ED-13,** 1966, p. 164.
39. R. J. McIntyre, ''The Distribution of Gains in Uniformly Multiplying Avalanche Photodiodes: Theory'', *IEEE Trans. Electron Devices,* **ED-19,** 1972, pp. 703–713.
40. S. D. Personick, ''Statistics of a General Class of Avalanche Detectors with Applications to Optical Communications,'' *Bell System Technical Journal,* **50,** 1971, pp. 167–189.
41. R. K. Dodd, et al., *Solitons and Nonlinear Wave Equations,* Academic Press, Orlando, Fl., 1984.
42. A. Hasegawa, *Solitons in Optical Fibers,* Springer-Verlag, Berlin, 1989.
43. L. F. Mollenauer, R. H. Stolen, and J. P. Gordon, ''Experimental Observation of Picosecond Pulse Narrowing and Solitons in Optical Fibers,'' *Phys. Rev. Letters,* **45,** 1980, p. 1095.
44. L. F. Mollenauer, et al., ''Extreme Picosecond Pulse Narrowing by Means of Soliton Effect in Single-Mode Optical Fibers'', *Opt. Lett.,* **8,** 1983, p. 289.
45. L. F. Mollenauer, R. H. Stolen, and M. N. Islam, ''Experimental Demonstration of Soliton Propagation in Long Fibers: Loss Compensated by Raman Gain'', *Opt. Lett.,* **10,** 1985, p. 229.
46. J. P. Gordon and H. A. Haus, *Opt. Lett.,* **11,** 1986, p. 665
47. L. F. Mollenauer, J. P. Gordon, and S. G. Evangelides, ''The Sliding Frequency Guiding Filter—an Improved Form of Soliton Jitter Control,'' *Opt. Lett.,* **17,** 1992, p. 1575.
48. A. R. Chraplyvy and R. W. Tkach, *Electron. Lett.,* **22,** 1986, p. 1084.
49. I. Garrett and G. Jacobsen, ''Theoretical Anaylsis of Heterodyne Optical Receivers using Semiconductor Lasers of Non-negligible Linewidth,'' *J. Lightwave Technology,* **4,** 1986, p. 323.
50. B. Glance, ''Performance of Homodyne Detection of Binary PSK Optical Signals,'' *J. Lightwave Technology,* **4,** 1986, p. 228.
51. L. G. Kazovsky, ''Performance Analysis and Laser Linewidth Requirements for Optical PSK Heterodyne Communications,'' *J. Lightwave Technology,* **4,** 1986, p. 415.
52. K. Kikuchi, et al., *J. Lightwave Technology,* **2,** 1984, p. 1024.
53. T. Okoshi and K. Kikuchi, *Coherent Optical Fiber Communications,* Kluwer, Boston, 1988.
54. N. A. Olsson et al., ''400 Mbit/s 372 = Km Coherent Transmission Experiment,'' *Electron. Lett.,* **24,** 1988, p. 36.
55. E. G. Bryant et al., ''A 1.2 Gbit/s Optical FSK Field Trial Demonstration,'' *British Telecom Technology Journal,* **8,** 1990, p. 18.
56. T. Okoshi, ''Polarization-State Control Schemes for Heterodyne of Homodyne Optical Fiber Communications,'' *J. Lightwave Technology,* **3,** 1985, pp. 1232–1237.

57. B. Glance, "Polarization Independent Coherent Optical Receiver," *J. Lightwave Technology,* **5,** 1987, p. 274.
58. R. H. Stolen, "Nonlinear Properties of Optical Fibers," in S. E. Miller and A. G. Chynowth, eds., *Optical Fiber Telecommunications,* Academic Press, New York.
59. G. P. Agrawal, "Nonlinear Interactions in Optical Fibers," in G. P. Agrawal and R. W. Boyd, eds., *Contemporary Nonlinear Optics,* Academic Press, San Diego, CA, 1992.
60. G. P. Agrawal, *Nonlinear Fiber Optics,* Academic Press, San Diego, CA, 1989.
61. J. R. Bautista and R. M. Atkins, "The Formation and Deposition of SiO_2 Aerosols in Optical Fiber Manufacturing Torches", *J. Aerosol Science,* **22,** 1991, pp. 667–675.
62. T. F. Morse, et al., "Aerosol Transport for Optical Fiber Core Doping: A New Technique for Glass Formation," *J. Aerosol Science,* **22,** 1991, pp. 657–666.
63. J. Nishii, et al., "Recent Advances and Trends in Chalcogenide Glass Fiber Technology: A Review," *J. Noncrystalline Solids,* **140,** 1992, pp. 199–208.
64. J. S. Sanghera, B. B. Harbison, and I. D. Aggarwal, "Challenges in Obtaining Low Loss Fluoride Glass Fibers," *J. Non-Crystalline Solids,* **140,** 1992, pp. 146–149.
65. S. Takahashi, "Prospects for Ultra-low Loss Using Fluoride Glass Optical Fiber," *J. Non-Crystalline Solids,* **140,** 1992, pp. 172–178.
66. I. Aggarwal, G. Lu, and L. Busse, *Materials Science Forum,* **32 & 33,** Plenum, New York, 1988, p. 495.

10.11 FURTHER READING

Agrawal, G. P., *Fiber-Optic Communication Systems,* John Wiley and Sons, New York, 1992.
Baack, C. (ed.), *Optical Wideband Transmission Systems,* CRC Press, Boca Raton, Fla., 1986.
Baker, D. G., *Fiber Optic Design and Applications,* Reston Publishing, Reston, Va., 1985.
Barnoski, M. K. (ed.), *Fundamentals of Optical Fiber Communications,* Academic Press, New York, 1981.
Basch, E. E. (ed.), *Optical Fiber Transmission,* Howard W. Sams, Indianapolis, 1987.
Chaffee, C. D., *The Rewiring of America*: *The Fiber Optics Revolution,* Academic Press, Boston, 1988.
Chaimowitz, J. C. A., *Lightwave Technology,* Butterworths, Boston, 1989.
Cheo, P. K., *Fiber Optics*: *Devices and Systems,* Prentice-Hall, Englewood Cliffs, NJ, 1985.
Cheo, P. K., *Fiber Optics and Optoelectronics,* Prentice-Hall, Englewood Cliffs, NJ, 1990.
Cherin, A. H., *An Introduction to Optical Fibers,* McGraw-Hill, 1983.
Culshaw, B., *Optical Fibre Sensing and Signal Processing,* Peter Peregrinus, London, 1984.
Daly, J. C., (ed.), *Fiber Optics,* CRC Press, Boca Raton, Fla., 1984.
Day, G. W., *Measurement of Optical-Fiber Bandwidth in the Frequency Domain,* NBS Special Publication, No. 637, National Bureau of Standards, Boulder, 1983.
Edwards, T. C., *Fiber-Optic Systems*: *Network Applications,* John Wiley and Sons, New York, 1989.
Geckeler, S., *Optical Fiber Transmission Systems,* Artech House, Norwood, Mass., 1987.
Gowar, J., *Optical Communications Systems,* Prentice-Hall, London, 1984.
Howes, M. J. and D. V. Morgan (ed.), *Optical Fiber Communications,* John Wiley and Sons, New York, 1980.
Jones, W. B., Jr., *Introduction to Optical Fiber Communications,* Holt, Rinehart and Winston, New York, 1988.
Kaiser, G. E., *Optical Fiber Communications,* McGraw-Hill, New York, 1991.
Kao, C. K., *Optical Fibre,* Peter Peregrinus, London, 1988.
Karp, S., R. Gagliardi, et al., *Optical Channels*: *Fibers, Clouds, Water, and the Atmosphere,* Plenum Press, New York, 1988.
Killen, H. B., *Fiber Optic Communications,* Prentice-Hall, Englewood Cliffs, NJ, 1991.

Li, T., (ed.), *Optical Fiber Data Transmission,* Academic Press, Boston, 1991.

Lin, C. (ed.), *Optoelectronic Technology and Lightwave Communications Systems,* Van Nostrand Reinhold, New York, 1989.

Mahlke, G. and P. Gossing, *Fiber Optic Cables,* John Wiley and Sons, New York, 1987.

Miller, S. E. and J. P. Kaminow (eds.), *Optical Fiber Telecommunications II,* Academic Press, San Diego, Calif., 1988.

Okoshi, T. and K. Kikuchi, *Coherent Optical Fiber Communications,* Kluwer, Boston, 1988.

Palais, J. C., *Fiber-Optic Communications,* Prentice-Hall, Englewood Cliffs, NJ, 1988.

Personick, S. D., *Optical Fiber Transmission Systems,* Plenum, New York, 1981.

Personick, S. D., *Fiber Optics*: *Technology and Applications,* Plenum Press, New York, 1985.

Runge, P. K. and P. R. Trischitta (eds.), *Undersea Lightwave Communications,* IEEE Press, New York, 1986.

Senior, J. M., *Optical Fiber Communications,* Prentice-Hall, London, 1985.

Sharma, A. B., S. J. Halme, et al., *Optical Fiber Systems and Their Components,* Springer-Verlag, Berlin, 1981.

Sibley, M. J. N., *Optical Communications,* Macmillan, London, 1990.

Taylor, H. F. (ed.), *Fiber Optics Communications,* Artech House, Norwood, Mass., 1983.

Taylor, H. F. (ed.), *Advances in Fiber Optics Communications,* Artech House, Norwood, Mass., 1988.

Tsang, W. T. (ed.), *Lightwave Communications Technology,* Semiconductors and Semimetals. Academic Press, Orlando, Fla., 1985.

Fibers in Medicine

Harrington, J. A. (ed.), *Infrared Fiber Optics III,* SPIE, Bellingham, Wash., 1991.

Joffe, S. N., *Lasers in General Surgery,* Williams & Wilkins, Baltimore, 1989.

Katzir, A. (ed.), *Selected papers on optical fibers in medicine,* SPIE, Bellingham, Wash., 1990.

Katzir, A. (ed.), *Proc. Optical Fibers in Medicine VII,* Bellingham, Wash., SPIE, 1992.

Nonlinear Properties of Fibers

Agrawal, G. P., *Nonlinear Fiber Optics,* Academic Press, San Diego, Calif., 1989.

Agrawal, G. P., "*Nonlinear Interactions in Optical Fibers,*" in *Contemporary Nonlinear Optics,* Academic Press, San Diego, Calif., 1992.

Hasegawa, A., *Solitons in Optical Fibers,* Springer-Verlag, Berlin, 1989.